

Supporting information

Highly efficient thermally activated delayed fluorescent emitters with suppressed energy loss and fast reverse intersystem crossing process

Xiao Zhang,^{†a} Jiao-Yang Li,^{†a} Kai Zhang,^{†b} Lei Ding,^{*c} Chuan-Kui Wang,^{*b} Man-Keung Fung^{ad*} and Jian Fan^{ae*}

^a Institute of Functional Nano & Soft Materials (FUNSOM), Jiangsu Key Laboratory for Carbon-Based Functional Materials & Devices, Soochow University, 199 Ren'ai Road, Suzhou, 215123, Jiangsu, PR China

^b Shandong Province Key Laboratory of Medical Physics and Image Processing Technology, School of Physics and Electronics, Shandong Normal University, 250014 Jinan, China

^c College of Electrical and Information Engineering, Shaanxi University of Science and Technology, Xi'an, Shaanxi, 710021, China

^d Macao Institute of Materials Science and Engineering, Macau University of Science and Technology, Taipa 999078, Macau SAR, China

^e State Key Laboratory of Structural Chemistry, Fujian Institute of Research on Structure of Matter, Chinese Academy of Sciences, Fuzhou, Fujian 35002, China

E-mail: dinglei@sust.edu.cn, ckwang@sdnu.edu.cn, mkfung@suda.edu.cn,
jianfan@suda.edu.cn

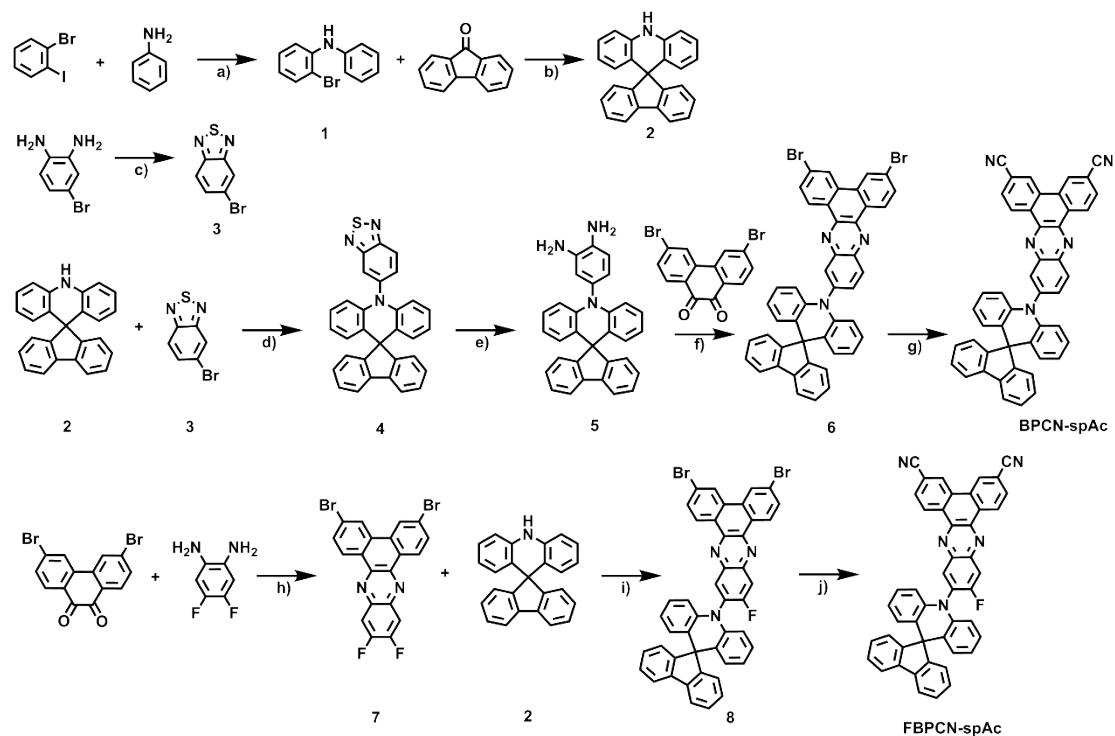
[†]These authors contribute equally to this work.

General Information

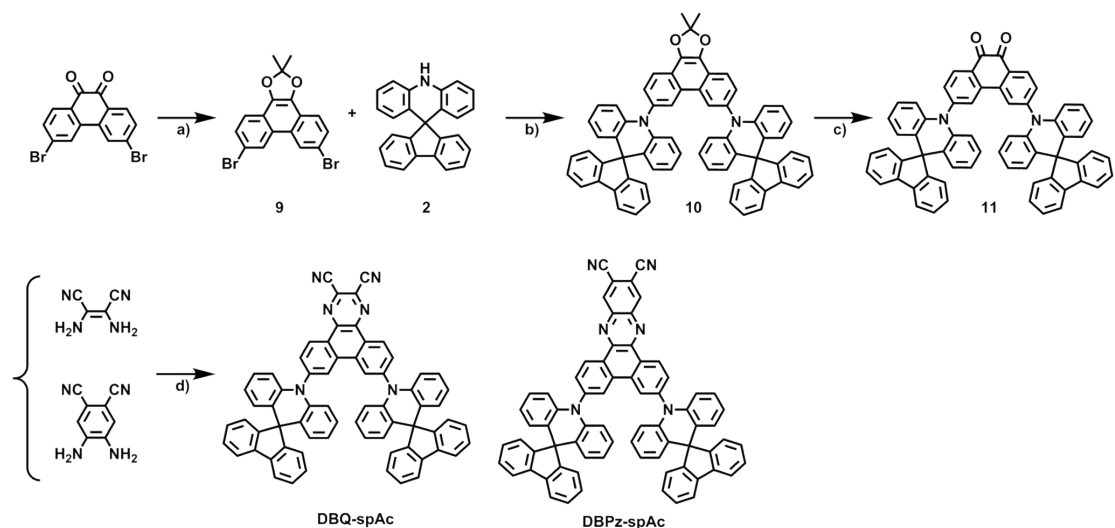
All chemicals and solvents were used as received unless otherwise stated. ^1H NMR nuclear magnetic resonance (NMR) spectra were performed on BRUKER400MHz or VNMR5300MHz. MALDI-TOF-MS (Matrix-Assisted Laser Desorption/Ionization Time of Flight Mass Spectrometry) were measured with a BRUKERr ultrafleXtreme MALDI-TOF spectrometer. UV-vis absorption spectra were obtained on a Hitachi U-3900 UV-Vis spectrophotometer. PL spectra and phosphorescent spectra were measured on a Hitachi F-4600 fluorescence spectrophotometer. PL lifetime spectra was obtained on Quantaaurus-Tau transient spectrometer (C11367-32, HAMAMATSU, Japan). Thermogravimetric analysis (TGA) was recorded on a TA SDT 2960 instrument at a heating rate of $5\text{ }^\circ\text{C min}^{-1}$ under nitrogen. Differential scanning calorimetry (DSC) was measured on a TA DSC 2010 unit at a heating rate of $5\text{ }^\circ\text{C min}^{-1}$ under nitrogen. Cyclic voltammetry (CV) was carried out on a CHI600 voltammetric analyzer at room temperature with ferrocenium-ferrocene (Fc^+/Fc) as the external standard. The scans were performed using $0.1\text{ M } n\text{-Bu}_4\text{NPF}_6$ (TBAPF_6) in oxygen-free dichloromethane solution.

Device Fabrication and Measurement

All the devices were fabricated on ITO glass substrates with the sheet resistance of $15\ \Omega\ \text{square}^{-1}$. The ITO glass substrates were cleaned by Decon and used ultrapure water and iso-Propyl alcohol for ultrasound for ten minutes respectively, dried using oven for two-three hours at a temperature of 100 degrees and exposed to UV-Ozone for 15minutes. OLED devices were prepared under the vacuum of 4×10^{-6} Torr. The deposition rate of hole-injection layer and electron-injection layer was $0.2\ \text{\AA}/\text{s}$ and the other organic layers was $2\text{-}4\ \text{\AA}/\text{s}$. The deposition rate of metal electrodes was $4\text{-}6\ \text{\AA}/\text{s}$. Device performance was measured by a Suzhou F-star Scientific Instrument. The photoluminescence spectra were obtained by a Hitachi F-4600 fluorescence spectrophotometer.



Scheme S1 Synthetic procedures of **BPCN-spAc** and **FBPCN-spAc**: a) $\text{Pd}_2(\text{dba})_3$, DPPF, $t\text{-BuONa}$, Tol, $100\text{ }^\circ\text{C}$, 12 h; b) $n\text{-BuLi}$, $-78\text{ }^\circ\text{C}$, 4h; RT, 12 h; MeSO_3H , CHCl_3 , 12 h; c) Py, SOCl_2 , $0\text{ }^\circ\text{C}\sim 70\text{ }^\circ\text{C}$, 5 h; d) $\text{Pd}_2(\text{dba})_3$, $\text{P}(t\text{-Bu})_3\text{H BF}_4$, $t\text{-BuONa}$, Tol, $120\text{ }^\circ\text{C}$, $65\text{ }^\circ\text{C}$, 12 h; e) LiAlH_4 , THF, $66\text{ }^\circ\text{C}$, 6 h; f/h) AcOH, $120\text{ }^\circ\text{C}$, 12 h; g/j) CuCN, NMP, $180\text{ }^\circ\text{C}$, 6 h; i) NaH, $80\text{ }^\circ\text{C}$, 12 h.



Scheme S2 Synthetic procedures of **DBQ-spAc** and **DBPz-spAc**: a) Na_2CO_3 , 2-nitropropane, $\text{H}_2\text{O} : \text{CH}_3\text{CN} = 1 : 1$, $80\text{ }^\circ\text{C}$, 4 h; b) $\text{Pd}_2(\text{dba})_3$, $\text{P}(t\text{-Bu})_3\text{H BF}_4$, $t\text{-BuONa}$, Tol, $120\text{ }^\circ\text{C}$, 12 h; c) TsOH, Tol, $100\text{ }^\circ\text{C}$, 4 h; d) AcOH, $120\text{ }^\circ\text{C}$, 12 h.

2-bromo-N-phenylaniline (1)

A mixture of aniline (4 g, 42.95 mmol), 1-bromo-2-iodobenzene (13.37 g, 47.2 mmol), t-BuONa (8.25 g, 85.90 mmol), Pd₂(dba)₃ (0.39g, 0.43 mmol) and DPPF (0.95g, 1.72 mmol) was dissolved in 80 mL dry toluene under nitrogen atmosphere. The reaction mixture was stirred at 100 °C for 12 h. After cooling to room temperature, the resulting solution was filtered through a Celite pad and to remove the precipitate, then concentrated under reduced pressure. The oil liquid product (10.22 g) was obtained by column chromatography with PE as the eluent. Yield: 96.3 %. ¹H NMR (300 MHz, DMSO-d₆) δ 7.59 (d, J = 7.9 Hz, 1H), 7.51 (s, 1H), 7.27 – 7.19 (m, 4H), 7.04 (d, J = 7.9 Hz, 2H), 6.91 – 6.82 (m, 2H).

10H-spiro[acridine-9,9'-fluorene] (2)

To a solution of compound 1 (4 g, 16.20 mmol) in dry THF (160 mL) at -78 °C under nitrogen atmosphere, n-BuLi (22.3 mL, 35.63 mmol, 1.6 M in hexane) was slowly added via syringe. Then this mixture was stirred for 4 hours at this temperature. 9H-fluoren-9-one (3.5 g, 19.44 mmol) was added to the solution for 30 minutes. The reaction system was allowed to stir for 12 hours at room temperature before the quenching with ice water. The solvent was removed under reduced pressure. The residue was extracted with CH₂Cl₂ and dried over Na₂SO₄. The resultant oil was dissolved in a mixture of CHCl₃ (100 mL) and methanesulfonic acid (1.2 mL, 17.82 mmol). Then the mixture was heated at 65 °C overnight before quenching the neutralization with NaHCO₃. The crude product was extracted three with CH₂Cl₂ and purified by column chromatography with PE/DCM (6/1, v/v) as the eluent. Yield: 43.47 %. ¹H NMR (300 MHz, DMSO-d₆) δ 9.24 (s, 1H), 7.91 (d, J = 7.5 Hz, 2H), 7.36 (t, J = 7.3 Hz, 2H), 7.26 – 7.14 (m, 4H), 6.99 (dd, J = 21.0, 7.6 Hz, 4H), 6.48 (t, J = 7.4 Hz, 2H), 6.10 (d, J = 7.8 Hz, 2H).

5-bromobenzo[c][1,2,5]thiadiazole (3)

To a solution of 4-bromobenzene-1,2-diamine (3 g, 16.04 mmol) in dry pyridine (50 mL) under nitrogen atmosphere, thionyl chloride (1.75 mL, 24.06 mmol) was added dropwise at 0 °C for 2 hours and then stirred at 70 °C for 3 hours. After cooling to room temperature, the resulting solution was carefully poured into ice water and filtered. The crude product was recrystallized from ethanol. Yield: 79.28 %. ¹H NMR

(400 MHz, CDCl₃-d) δ 8.23 (s, 1H), 7.89 (d, J = 9.0 Hz, 1H), 7.68 (d, J = 9.0 Hz, 1H).

5-(10H-spiro[acridine-9,9'-fluoren]-10-yl)benzo[c][1,2,5]thiadiazole (4)

Compound 3 (1.50 g, 7.01 mmol), 2 (2.55 g, 7.71 mmol), t-BuONa (1.35 g, 14.02 mmol), Pd₂(dba)₃ (128 mg, 0.14 mmol), P(t-Bu)₃H·BF₄ (162 mg, 0.56 mmol) were added to dry toluene (30 mL) under nitrogen, and then stirred at 120 °C for 12h. After cooling down to room temperature, the solvent was removed under reduced pressure, and then extracted three time with CH₂Cl₂. The crude product was purified by column chromatography with PE/DCM (3/1, v/v) as the eluent. Yield: 82.78 %. ¹H NMR (400 MHz, CDCl₃) δ 8.35 (dd, J = 9.1, 0.8 Hz, 1H), 8.28 (dd, J = 1.9, 0.8 Hz, 1H), 7.82 (dt, J = 7.5, 0.9 Hz, 2H), 7.69 (dd, J = 9.1, 2.0 Hz, 1H), 7.47 – 7.36 (m, 4H), 7.29 (dd, J = 7.4, 1.2 Hz, 2H), 6.93 (ddd, J = 8.5, 7.2, 1.6 Hz, 2H), 6.62 (ddd, J = 8.2, 7.2, 1.2 Hz, 2H), 6.44 (ddd, J = 11.3, 8.1, 1.4 Hz, 4H).

4-(10H-spiro[acridine-9,9'-fluoren]-10-yl)benzene-1,2-diamine (5)

To a stirred solution of compound 4 (2.70 g, 5.80 mmol) in dry THF (40 mL) under nitrogen, a solution of LiAlH₄ (1.52 g, 40 mmol) in dry THF (20 mL) was added dropwise at 0 °C. After stirring for 20 min, the reaction mixture was refluxed overnight. The reaction mixture was quenched by the addition of ice water. The precipitate was collected by the filtration. The crude product was purified by column chromatography with DCM as the eluent. Yield: 57.55 %. ¹H NMR (400 MHz, DMSO-d₆) δ 7.95 (d, J = 7.5 Hz, 2H), 7.40 (t, 2H), 7.29 (d, J = 15.0 Hz, 4H), 6.94 (s, 2H), 6.81 (d, J = 8.0 Hz, 1H), 6.60 (d, 1H), 6.56 – 6.43 (m, 5H), 6.18 (dd, J = 8.7 Hz, 2H), 4.81 (s, 4H).

10-(3,6-dibromodibenzo[a,c]phenazin-11-yl)-10H-spiro[acridine-9,9'-fluorene](6)

Compound 5 (1.46 g, 3.34mmol) and 3,6-dibromophenanthrene-9,10-dione (1.28 g, 3.51mmol) in AcOH (40 mL) was heated at 120 °C overnight under nitrogen. The crude product was washed with water and recrystallized in ethanol (2.07 g). Yield: 81.01 %. ¹H NMR (400 MHz, CDCl₃) δ 9.35 (d, J = 8.6 Hz, 1H), 9.29 (d, J = 8.6 Hz, 1H), 8.66 (d, J = 8.7 Hz, 3H), 8.57 (d, J = 2.3 Hz, 1H), 8.01 – 7.90 (m, 3H), 7.84 (d, J = 7.5 Hz, 2H), 7.54 – 7.50 (m, 2H), 7.42 (dd, J = 7.9, 6.7 Hz, 2H), 7.35 (d, J = 2.7 Hz, 2H), 7.08 (dd, J = 8.4, 2.5 Hz, 2H), 6.95 – 6.89 (m, 2H), 6.62 (t, J = 7.4 Hz, 2H), 6.50 – 6.47 (m, 2H).

BPCN-spAc

Compound 5 (1g, 1.31mmol) and CuCN (294mg, 3.28mmol) were suspended in 1-methyl-2-pyrrolidinone (20 mL). This reaction was carried out at 180 °C under microwave for 6 h. Then the solvent was removed under reduced pressure. The crude product was washed with aqueous solution of ferric chloride and then purified by column chromatography with PE/CH₂Cl₂ (3/2, v/v) as the eluent (431 mg). Yield: 47.83 %. ¹H NMR (400 MHz, CDCl₃) δ 9.65 (dd, J = 23.2, 8.4 Hz, 2H), 8.92 (s, 2H), 8.75 (d, J = 9.0 Hz, 1H), 8.68 (d, J = 2.2 Hz, 1H), 8.17 – 8.08 (m, 3H), 7.87 (d, J = 7.5 Hz, 2H), 7.54 (d, J = 7.5 Hz, 2H), 7.45 (t, J = 7.4 Hz, 2H), 7.35 (t, J = 7.4 Hz, 2H), 6.96 (dd, J = 8.5, 7.1 Hz, 2H), 6.67 (t, J = 7.5 Hz, 2H), 6.51 (t, J = 8.1 Hz, 4H). MALDI-TOF-MS: m/z calcd for C₄₇H₂₅N₅:659.21, found: 659.100.

3,6-dibromo-11,12-difluorodibenzo[a,c]phenazine (7)

The synthetic procedure of compound 7 was similar to that for compound 6. Purple solid (Yield: 73.86 %). ¹H NMR (400 MHz, C₆D₄Cl₂) δ 9.28 (d, J = 8.5 Hz, 2H), 8.52 (s, 2H), 8.06 (t, J = 10.5 Hz, 2H), 7.92 (d, J = 8.4 Hz, 2H).

10-(3,6-dibromo-12-fluorodibenzo[a,c]phenazin-11-yl)-10H-spiro[acridine-9,9'-fluorene] (8)

Compound 7 (0.5 g, 1.06 mmol), 2 (0.37 g 1.11 mmol) and NaH (51 mg, 2.12 mmol) were added to dry DMF (20 mL) under nitrogen, and then this mixture was stirred at 80 °C for 12h. After the removal of the solvent, the residue was extracted with CH₂Cl₂. The crude product was purified by column chromatography with PE/DCM (4/1, v/v) as the eluent (500 mg). Yield: 60.28 % ¹H NMR (400 MHz, CDCl₃) δ 9.33 (d, J = 8.6 Hz, 1H), 9.26 (d, J = 8.6 Hz, 1H), 8.70 – 8.62 (m, 3H), 8.31 (d, J = 9.9 Hz, 1H), 7.93 (ddd, J = 10.7, 8.6, 1.8 Hz, 2H), 7.84 (d, J = 7.5 Hz, 2H), 7.55 – 7.50 (m, 2H), 7.44 – 7.38 (m, 2H), 7.32 (d, J = 7.1 Hz, 2H), 6.96 (ddd, J = 8.6, 7.2, 1.6 Hz, 2H), 6.65 (td, J = 7.6, 1.1 Hz, 2H), 6.55 – 6.45 (m, 4H).

FBPCN-spAc

The synthetic procedure for compound FBPCN-spAc was similar to that for compound BPCN-spAc. Red solid (260 mg, Yield: 63.56 %). ¹H NMR (400 MHz, CDCl₃) δ 9.63 (d, J = 8.4 Hz, 1H), 9.56 (d, J = 8.3 Hz, 1H), 8.91 (s, 2H), 8.74 (d, J =

7.8 Hz, 1H), 8.38 (d, $J = 9.7$ Hz, 1H), 8.15 – 8.07 (m, 2H), 7.84 (d, $J = 7.4$ Hz, 2H), 7.50 (s, 2H), 7.42 (t, $J = 7.4$ Hz, 2H), 7.32 (t, $J = 7.4$ Hz, 2H), 6.96 (t, $J = 7.7$ Hz, 2H), 6.67 (t, $J = 7.5$ Hz, 2H), 6.49 (dd, $J = 8.1, 5.0$ Hz, 4H). MALDI-TOF-MS: m/z calcd for $C_{47}H_{25}FN_5$: 677.20, found: 677.088.

6,9-dibromo-2,2-dimethylphenanthro[9,10-d][1,3]dioxole (9)

A mixture of 3,6-dibromophenanthrene-9,10-dione (2 g, 5.46 mmol) and 2-nitropropane (48.6 g, 546 mmol) in $H_2O:CH_3CN$ ($v:v = 1:1$, 200 mL) was stirred for 5 minutes before the addition of Na_2CO_3 (607 mg, 5.57 mmol). Then the mixture was refluxed for 4 hours. After cooling to room temperature, the solvent was removed under reduced pressure. The crude product was purified by column chromatography with PE/DCM (4/1, v/v) as the eluent (1.58 g). Yield: 71.02 %. 1H NMR (400 MHz, $DMSO-d_6$) δ 9.17 (d, $J = 1.7$ Hz, 2H), 7.83 (d, 2H), 7.78 (s, 2H), 1.83 (s, 6H).

10,10''-(2,2-dimethylphenanthro[9,10-d][1,3]dioxole-6,9-diyl)bis(10H-spiro[acridine-9,9'-fluorene]) (10)

The synthetic procedure for compound 10 was similar to that for compound 4. Yellow solid (2.23 g, Yield: 63.20 %). 1H NMR (400 MHz, $CDCl_3$) δ 8.77 (s, 2H), 8.33 (d, $J = 8.6$ Hz, 2H), 7.79 (dd, $J = 11.6, 8.0$ Hz, 6H), 7.48 (d, $J = 7.5$ Hz, 4H), 7.38 (t, $J = 7.4$ Hz, 4H), 7.29 (s, 4H), 6.87 (t, $J = 7.8$ Hz, 4H), 6.55 (t, $J = 7.5$ Hz, 4H), 6.39 (dd, $J = 12.3, 8.1$ Hz, 8H), 2.01 (s, 6H).

3,6-di(10H-spiro[acridine-9,9'-fluoren]-10-yl)phenanthrene-9,10-dione (11)

To a stirred solution of compound 11 (1.41g, 1.55 mmol) in toluene (40 mL), TsOH (30 mg, 0.16 mmol) was added at room temperature. The reaction mixture was refluxed for 4 hours. The resulting solution was washed with water, and the organic solvent was removed under reduced pressure. The crude product was purified by column chromatography silica with PE/DCM (2/3, v/v) as the eluent (1.3 g). Yield: 97 %. 1H NMR (300 MHz, $CDCl_3$) δ 8.66 (d, $J = 8.2$ Hz, 2H), 8.17 (s, 2H), 7.77 (dd, $J = 23.3, 7.8$ Hz, 6H), 7.37 (t, $J = 7.5$ Hz, 8H), 7.25 – 7.16 (m, 6H), 6.95 (t, $J = 8.1$ Hz, 4H), 6.61 (t, $J = 7.5$ Hz, 4H), 6.49 – 6.38 (m, 6H).

DBQ-spAc

The synthetic procedure for compound DBQ-spAc was similar to that for compound 6.

Red solid (120 mg, Yield: 52.63 %). ^1H NMR (400 MHz, CD_2Cl_2) δ 9.64 (d, $J = 8.5$ Hz, 1H), 8.84 (d, $J = 1.9$ Hz, 1H), 8.06 (dd, $J = 8.6, 1.8$ Hz, 1H), 7.86 (dt, $J = 7.5, 0.9$ Hz, 2H), 7.48 – 7.37 (m, 4H), 7.28 (td, $J = 7.5, 1.2$ Hz, 2H), 6.91 (ddd, $J = 8.5, 7.1, 1.6$ Hz, 2H), 6.59 (td, $J = 7.5, 1.2$ Hz, 2H), 6.41 (td, $J = 7.9, 7.5, 1.4$ Hz, 4H). MALDI-TOF-MS: m/z calcd for $\text{C}_{68}\text{H}_{38}\text{N}_6$: 938.32, found: 938.136.

DBPz-spAc

The synthetic procedure for compound DBPz-spAc was similar to that for compound 6. Red solid (120 mg, Yield: 58.46 %). ^1H NMR (400 MHz, CD_2Cl_2) δ 9.83 (d, $J = 8.5$ Hz, 1H), 8.98 (s, 1H), 8.76 (d, $J = 2.0$ Hz, 1H), 8.02 (dd, $J = 8.4, 1.8$ Hz, 1H), 7.86 (d, $J = 7.5$ Hz, 2H), 7.52 – 7.36 (m, 4H), 7.28 (td, $J = 7.4, 1.1$ Hz, 2H), 6.91 (ddd, $J = 8.6, 7.2, 1.7$ Hz, 2H), 6.63 – 6.53 (m, 2H), 6.48 (dd, $J = 8.4, 1.1$ Hz, 2H), 6.40 (dd, $J = 7.9, 1.6$ Hz, 2H). MALDI-TOF-MS: m/z calcd for $\text{C}_{72}\text{H}_{40}\text{N}_6$: 988.33, found: 988.149.

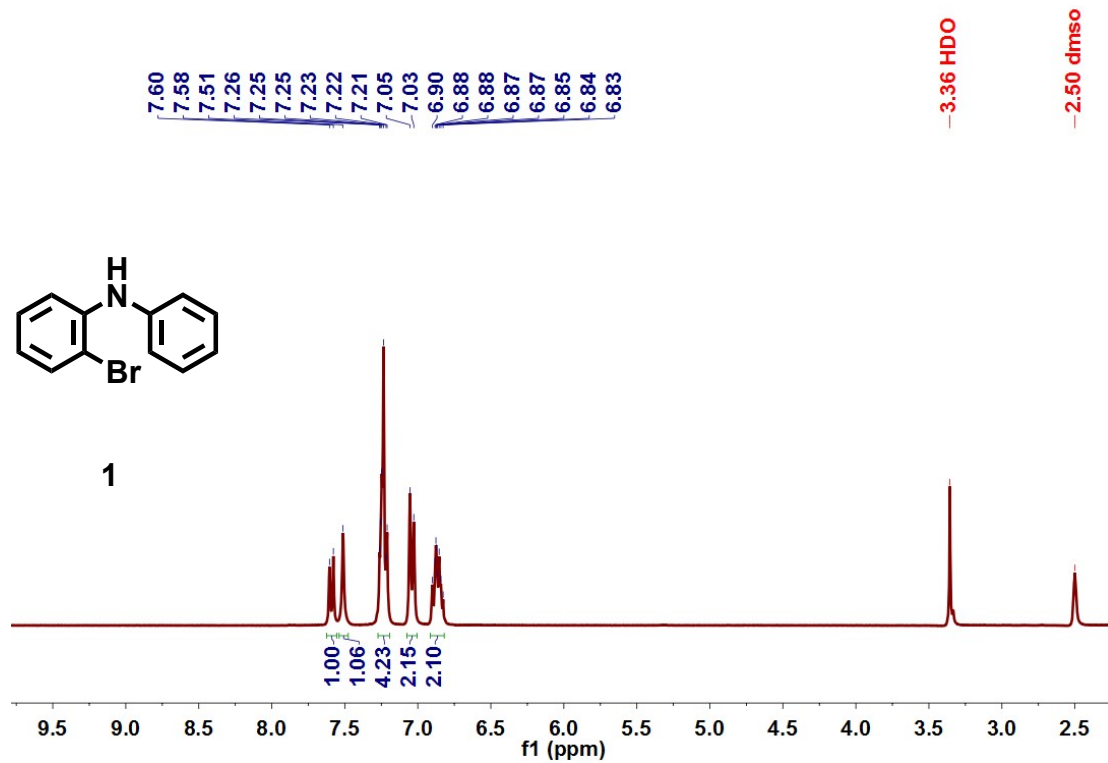


Figure S1 ¹H NMR spectrum (DMSO-*d*₆, 300 MHz) of compound 1.

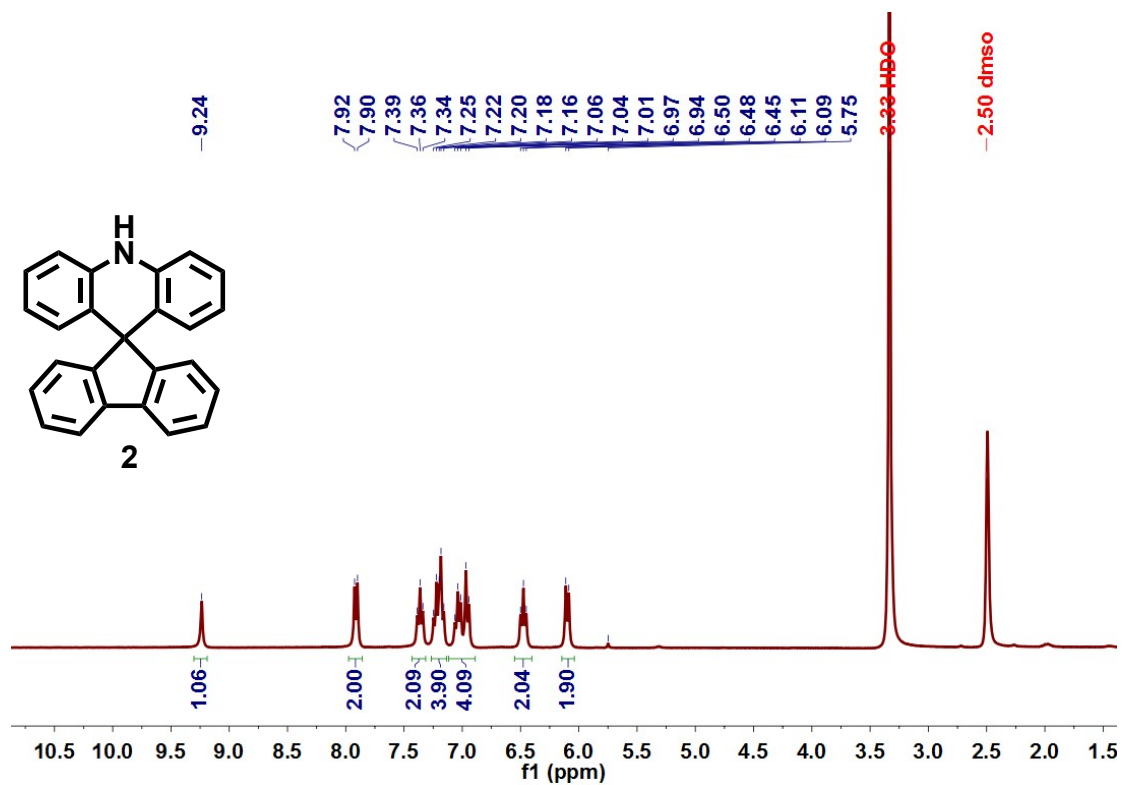


Figure S2 ¹H NMR spectrum (DMSO-*d*₆, 300 MHz) of compound 2.

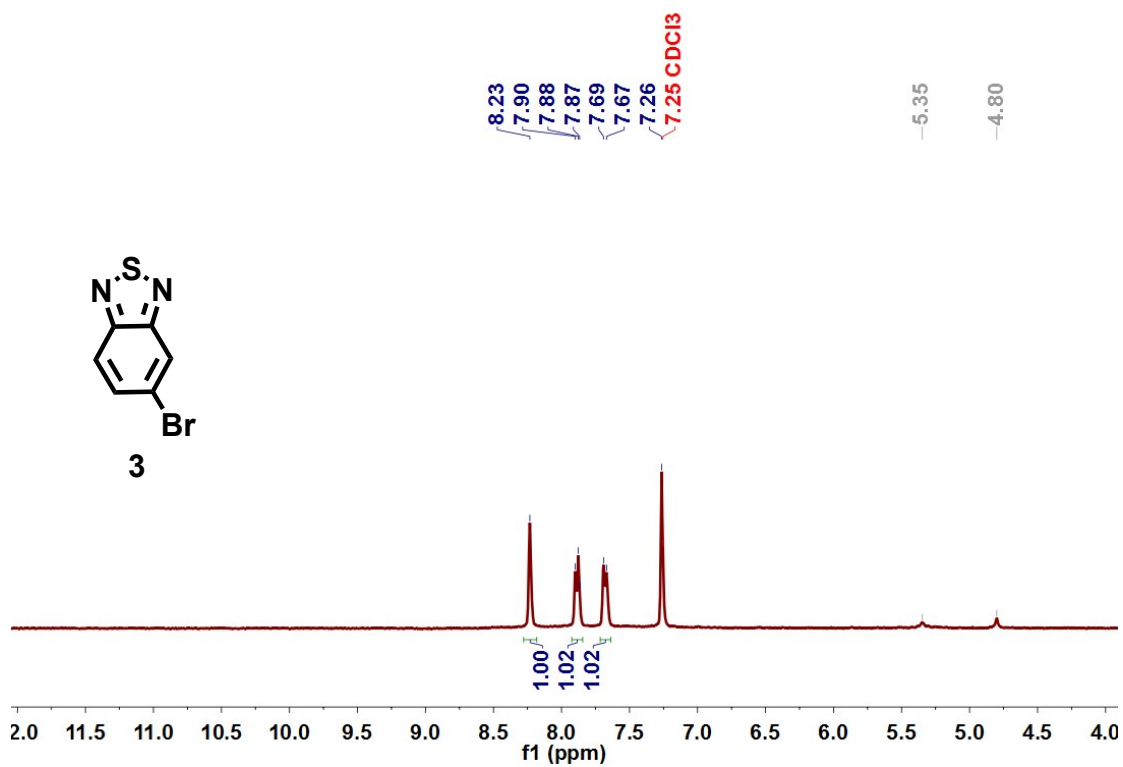


Figure S3 ¹H NMR spectrum (CDCl₃, 400 MHz) of compound 3.

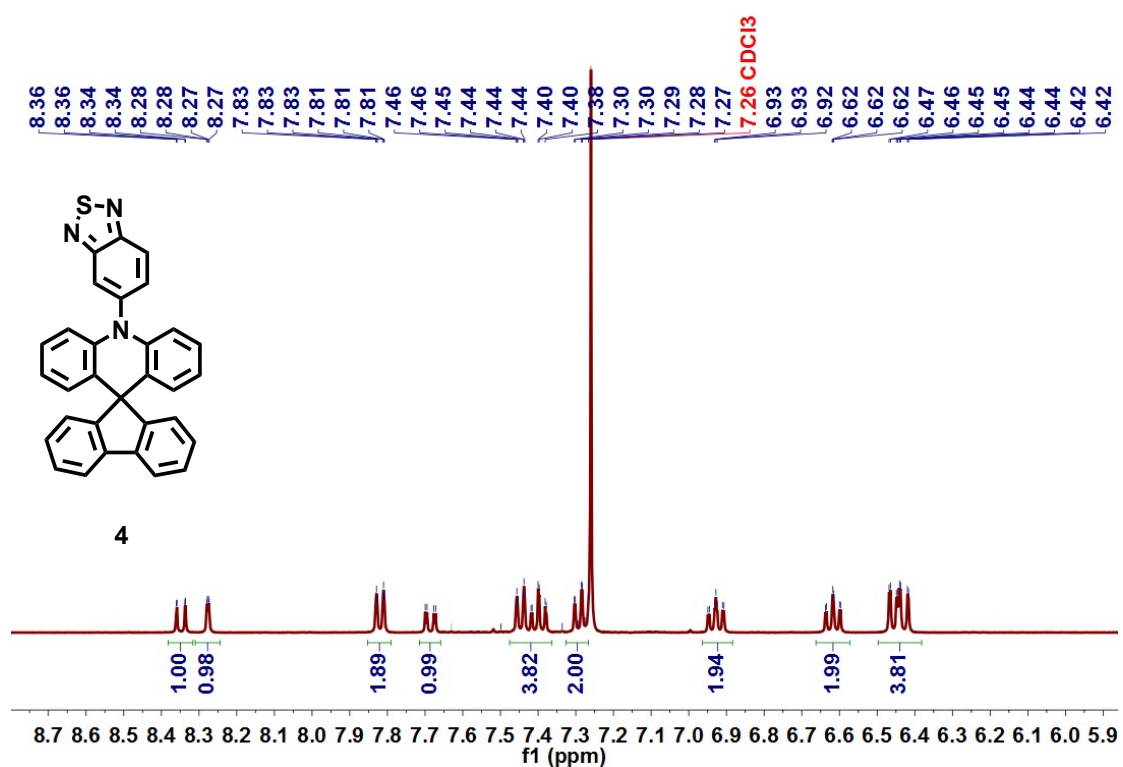


Figure S4 ¹H NMR spectrum (CDCl₃, 400 MHz) of compound 4.

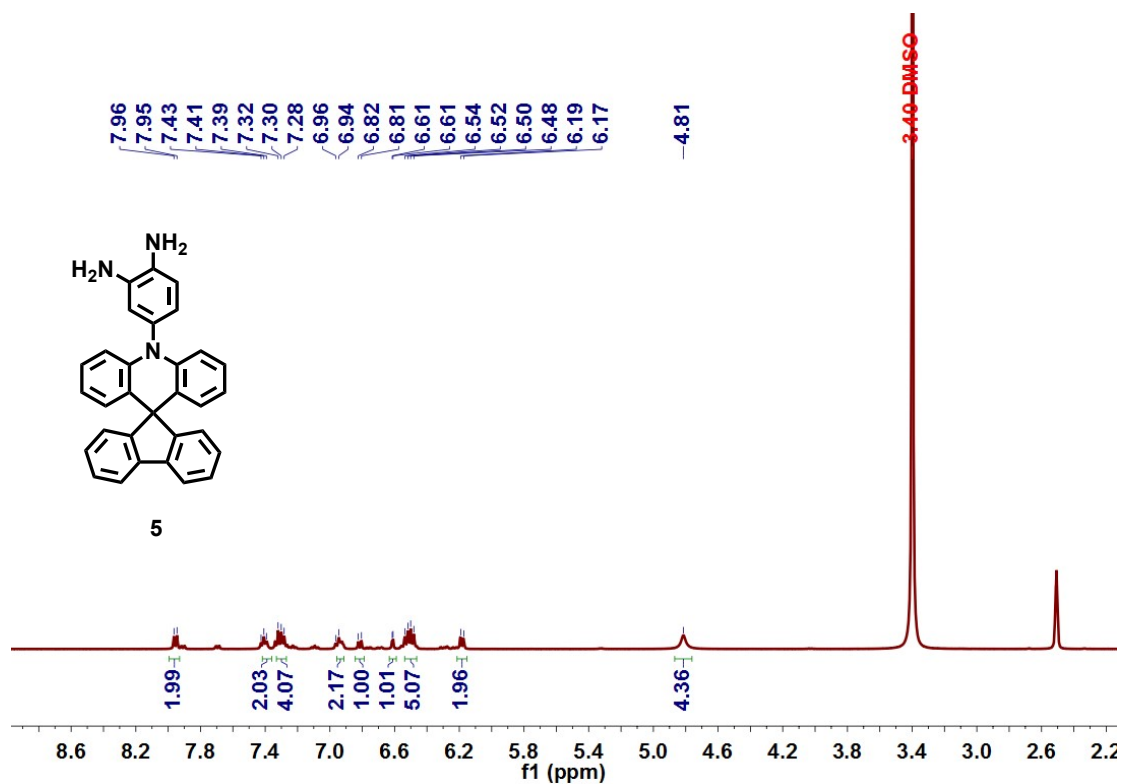


Figure S5 ¹H NMR spectrum (DMSO-*d*₆, 400 MHz) of compound 5.

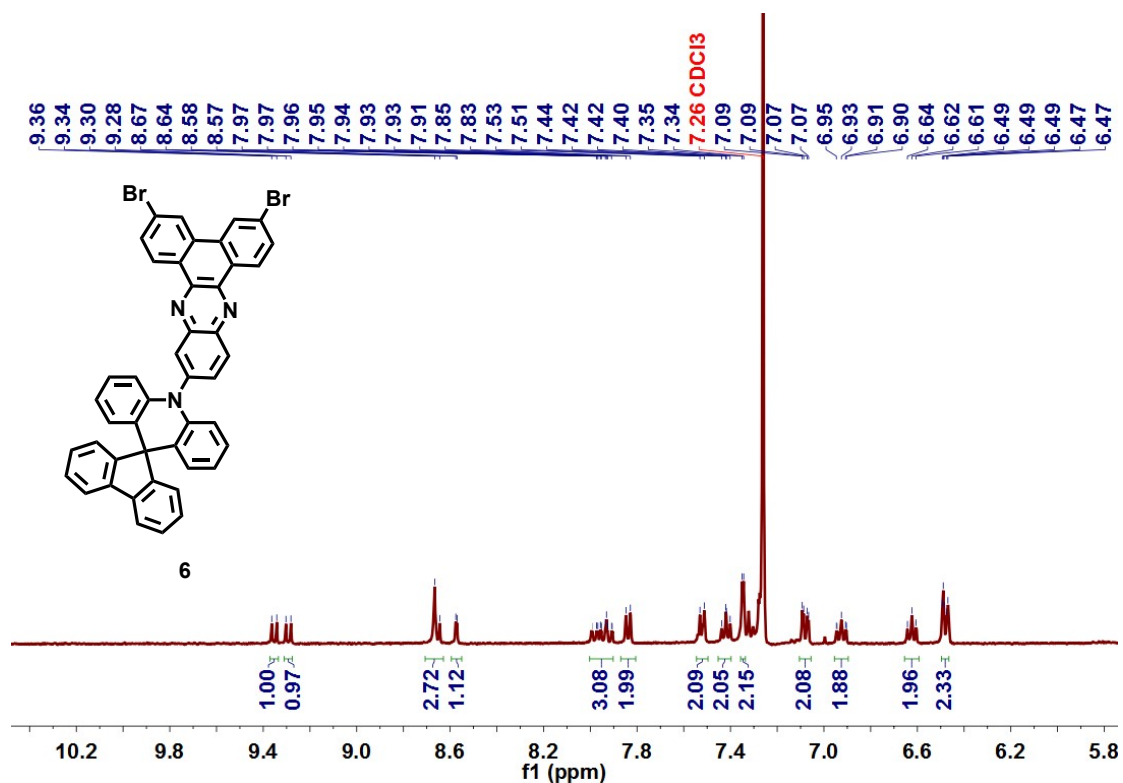


Figure S6 ¹H NMR spectrum (CDCl₃, 400 MHz) of compound 6.

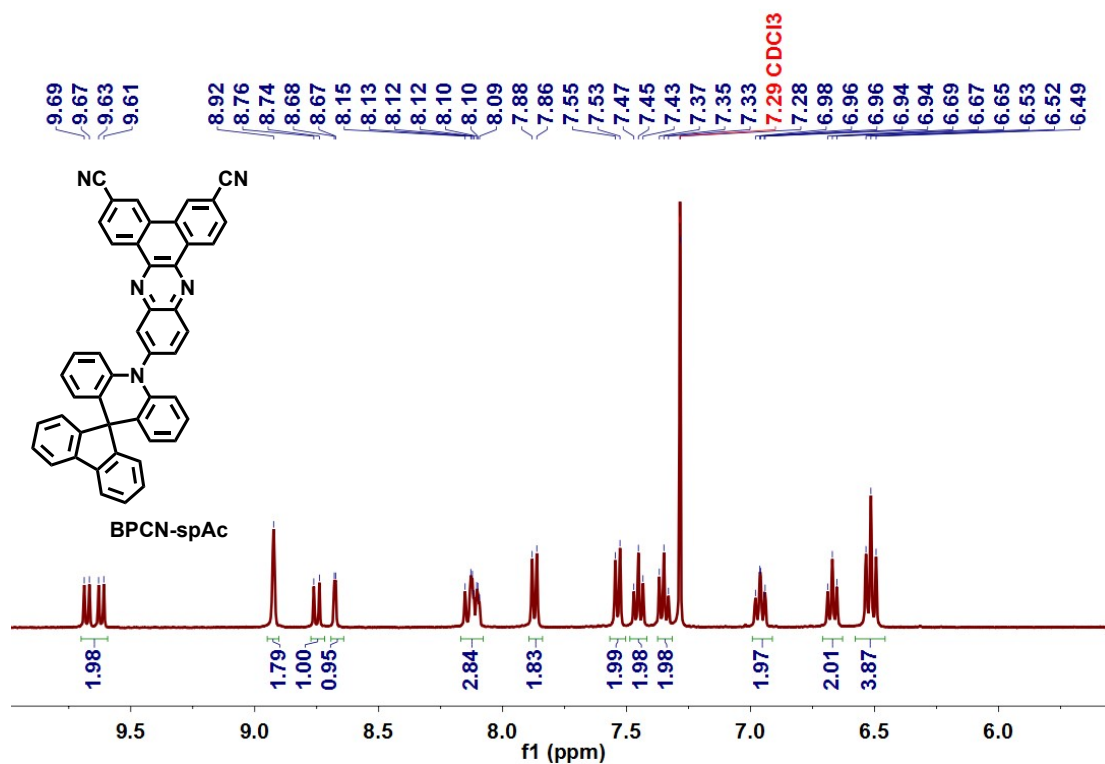


Figure S7 ¹H NMR spectrum (CD₂Cl₂, 400 MHz) of BPCN-spAc.

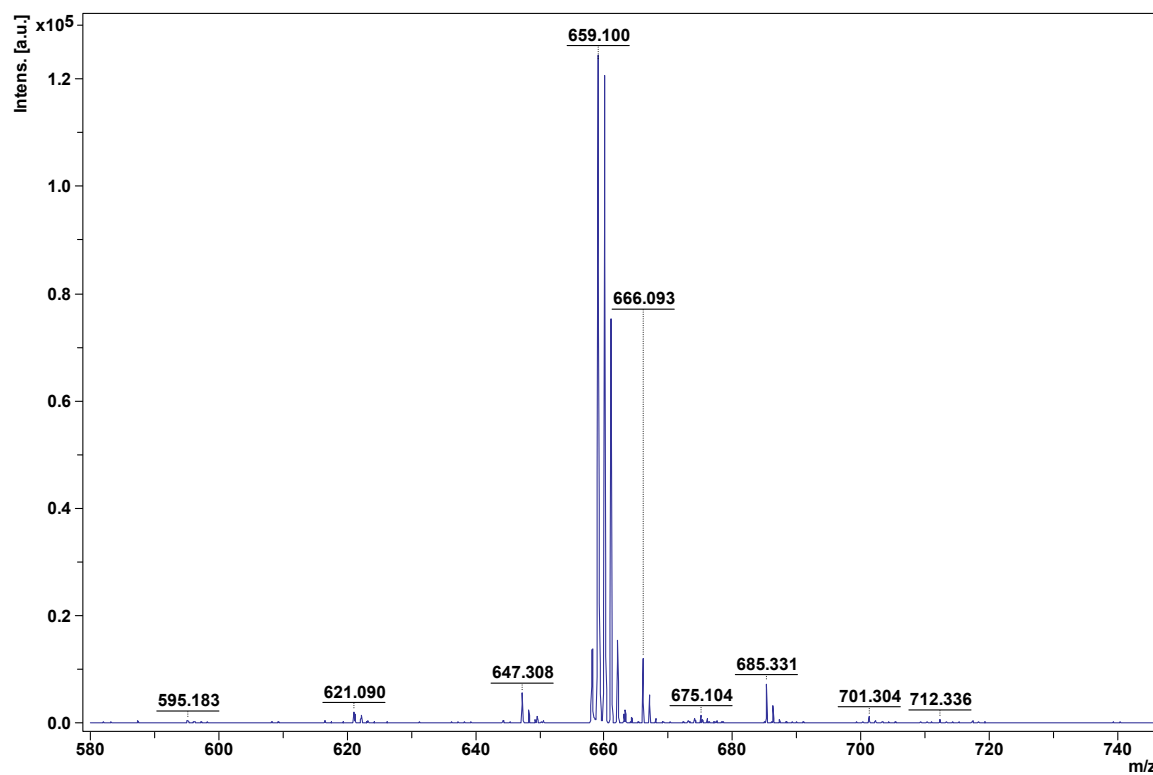


Figure S8 MALDI-TOF mass spectrum of BPCN-spAc.

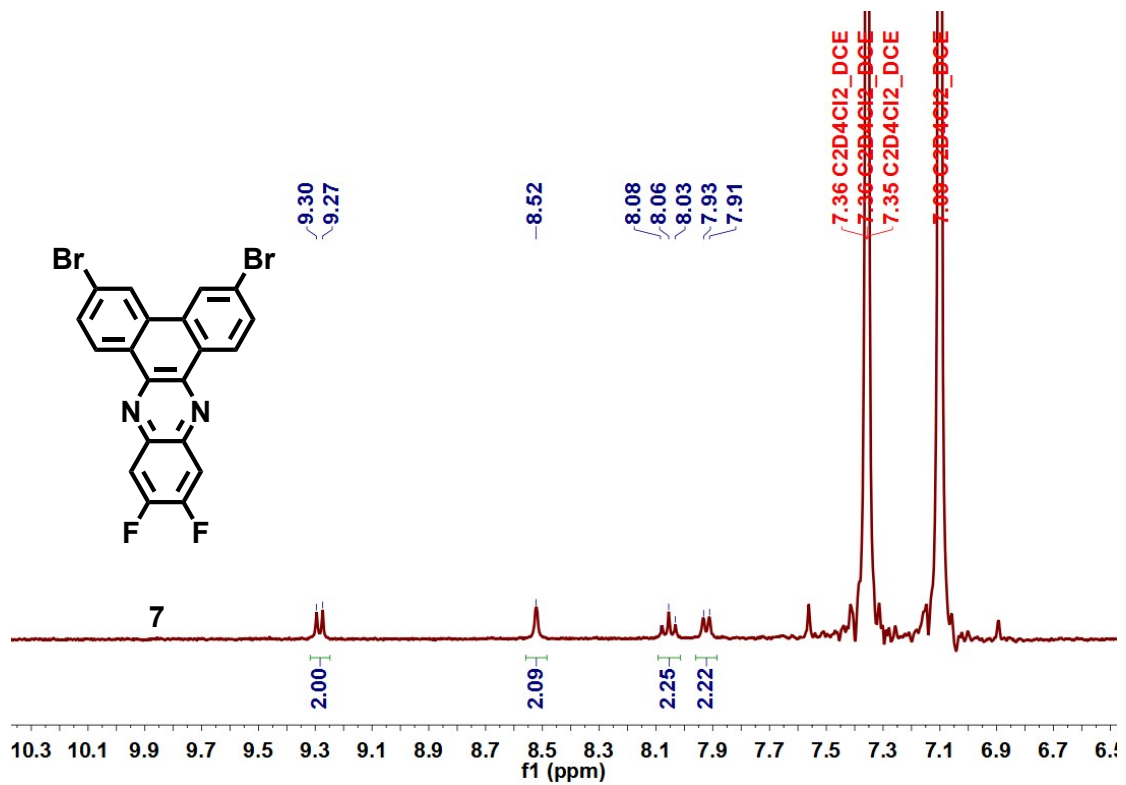


Figure S9 ¹H NMR spectrum (C₆D₄Cl₂, 400 MHz) of compound 7.

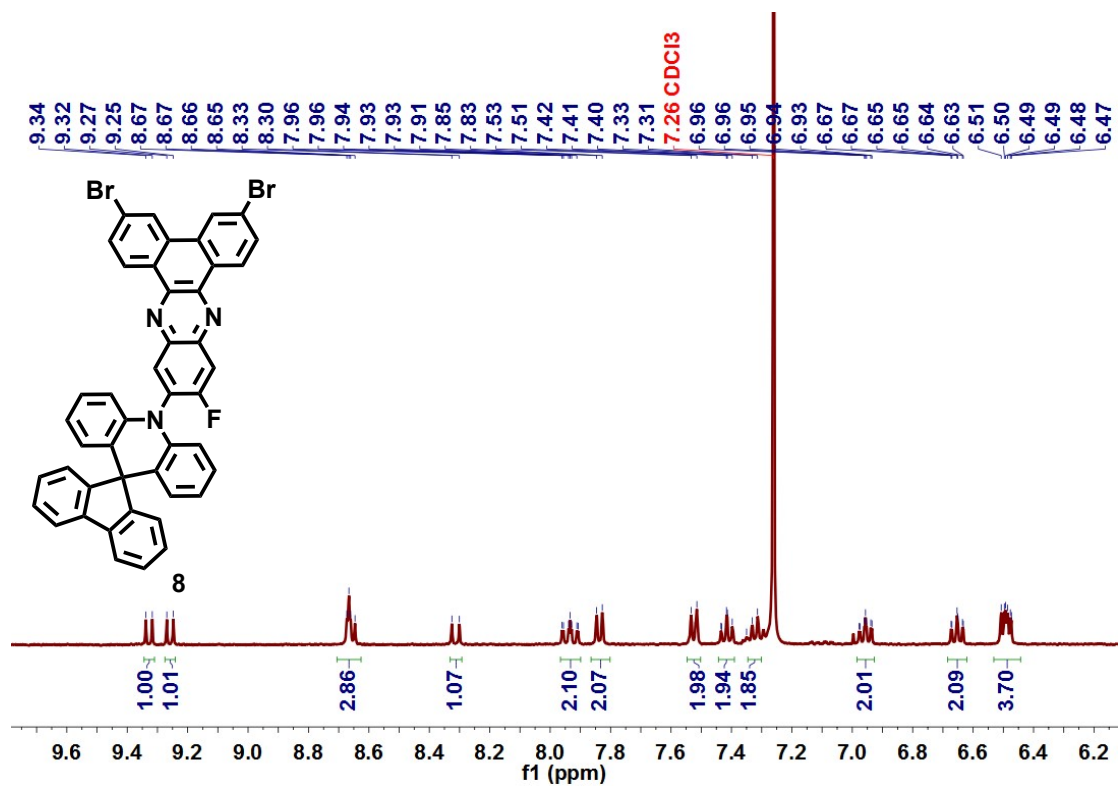


Figure S10 ¹H NMR spectrum (CDCl₃, 400 MHz) of compound 8.

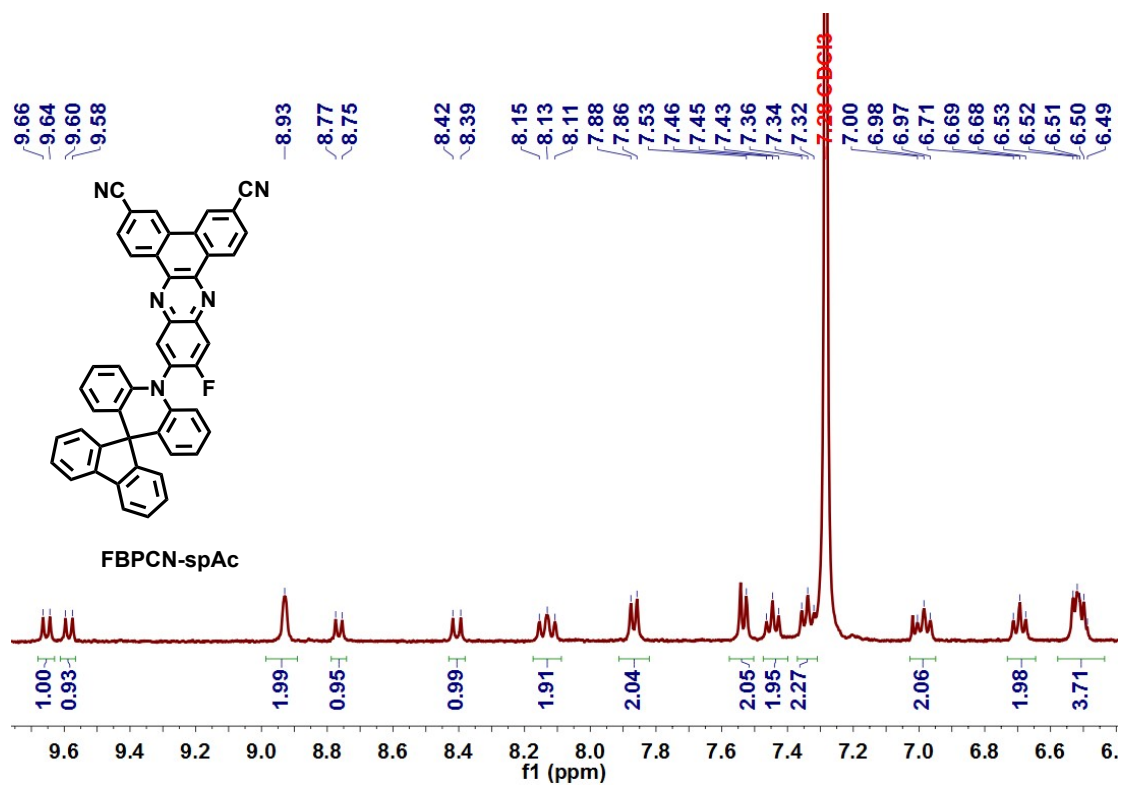


Figure S11 ¹H NMR spectrum (CDCl₃, 400 MHz) of FBPCN-spAc.

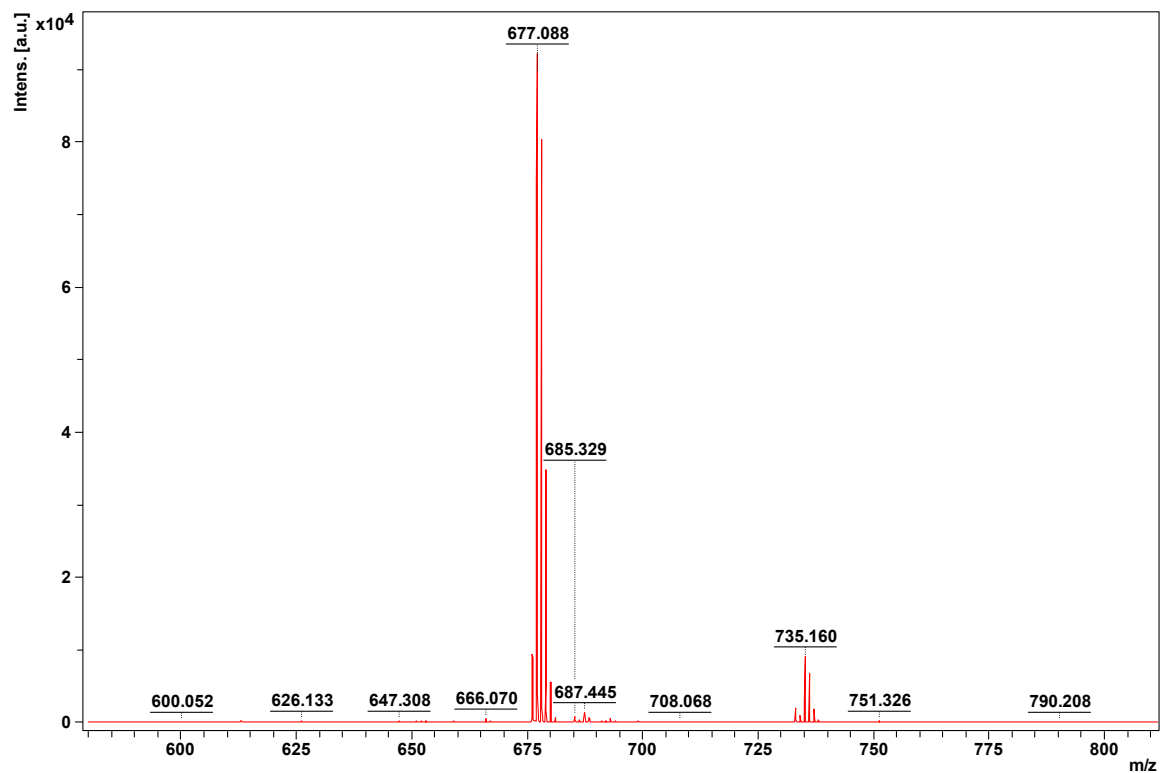


Figure S12 MALDI-TOF mass spectrum of FBPCN-spAc.

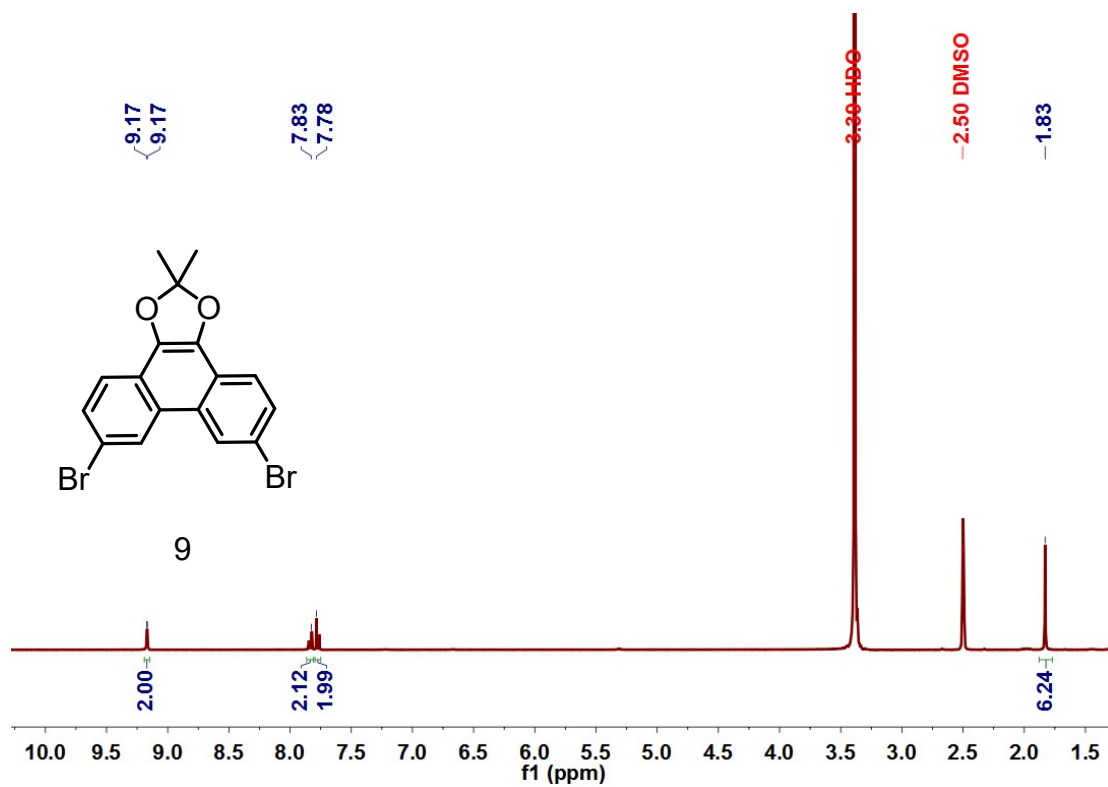


Figure S13 ¹H NMR spectrum (DMSO-*d*₆, 400 MHz) of compound 9.

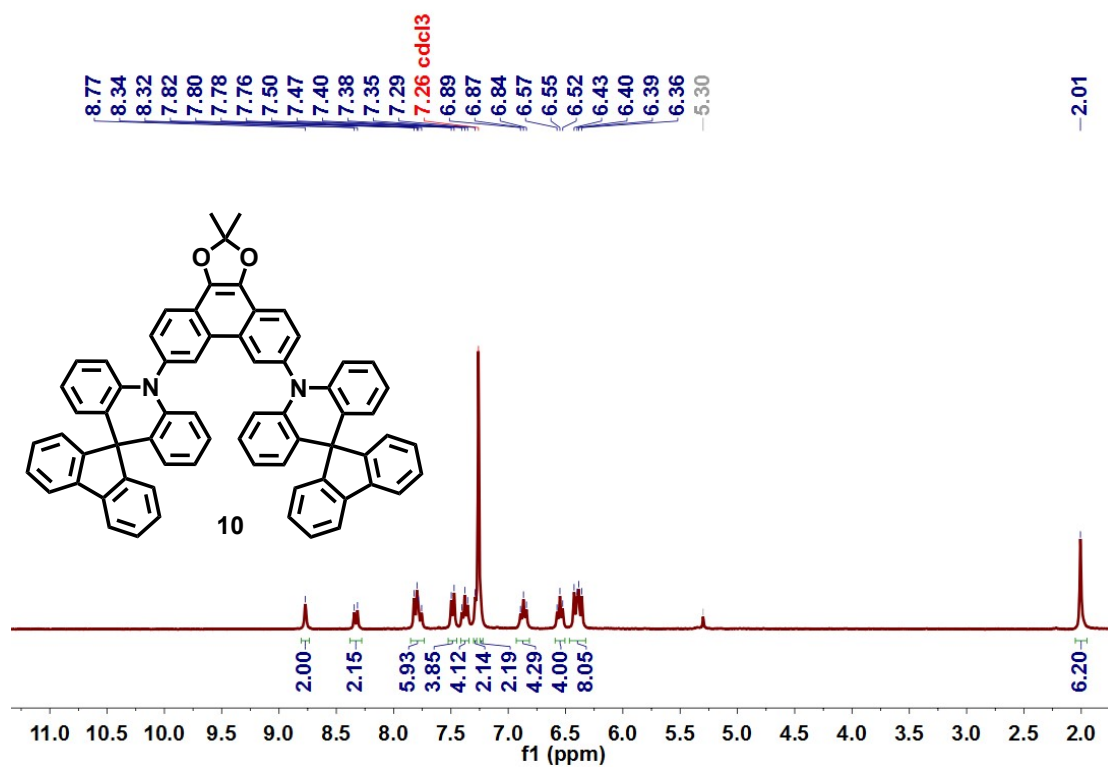


Figure S14 ¹H NMR spectrum (CDCl₃, 400 MHz) of compound 10.

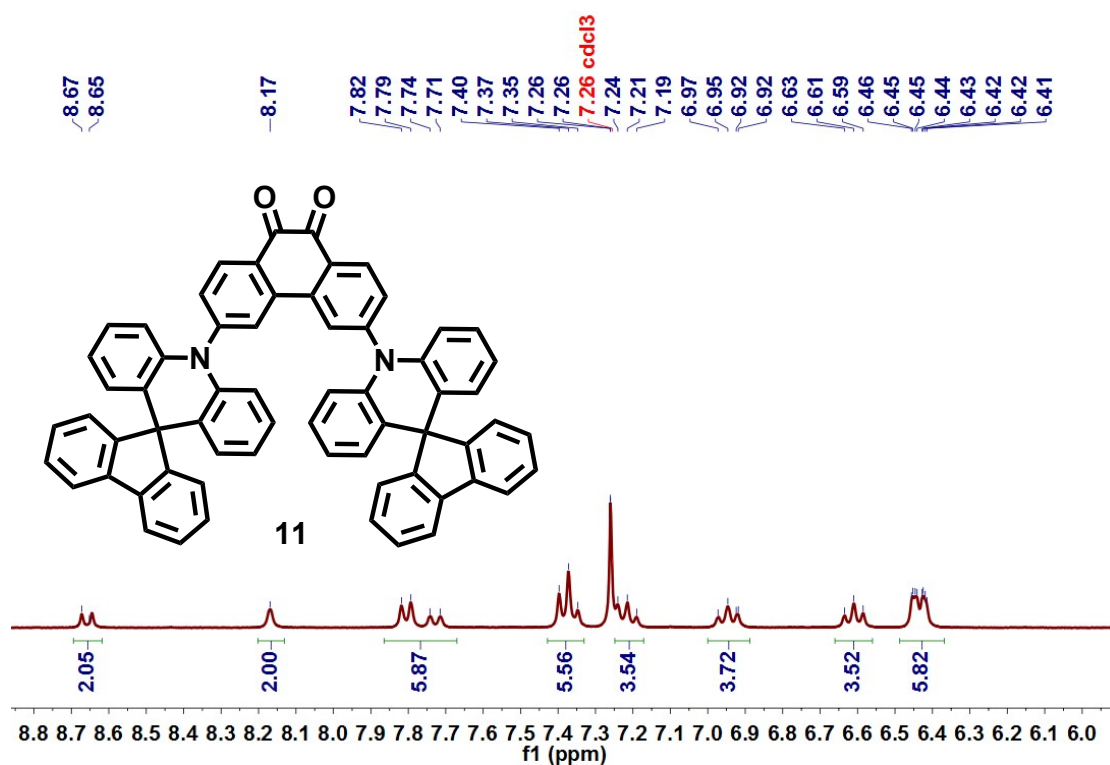


Figure S15 ¹H NMR spectrum (CDCl₃, 400 MHz) of compound 11.

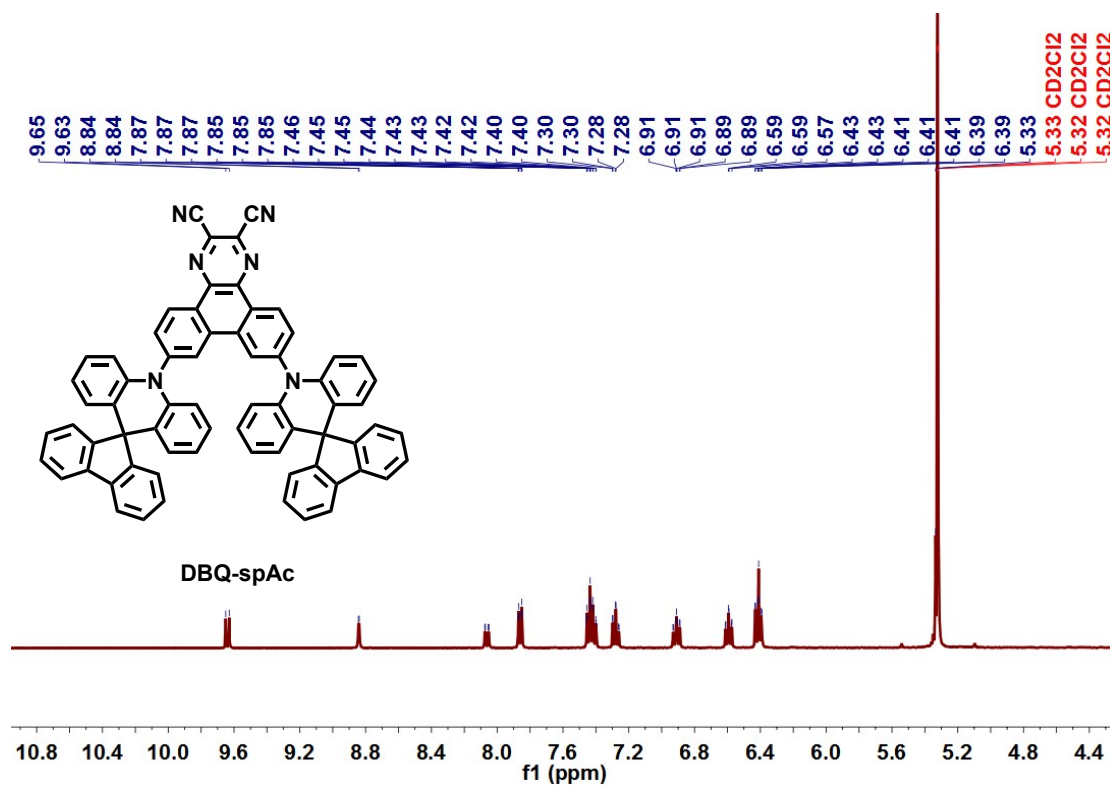


Figure S16 ¹H NMR spectrum (CD₂Cl₂, 400 MHz) of DBQ-spAc.

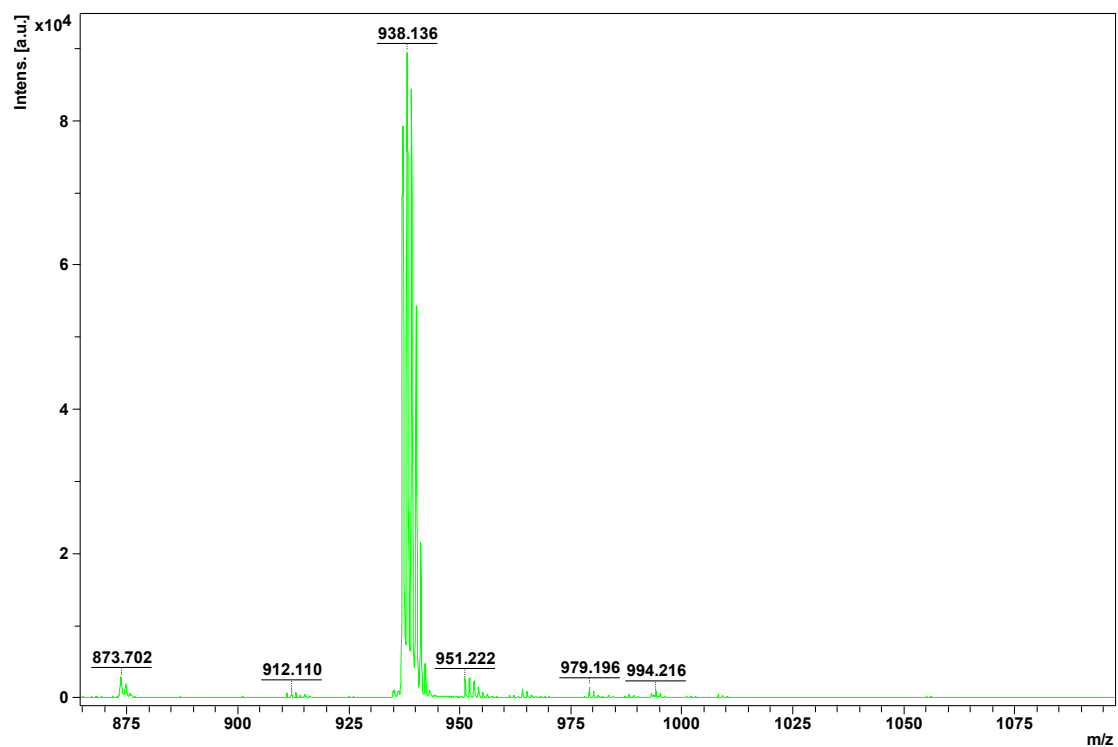


Figure S17 MALDI-TOF mass spectrum of DBQ-spAc.

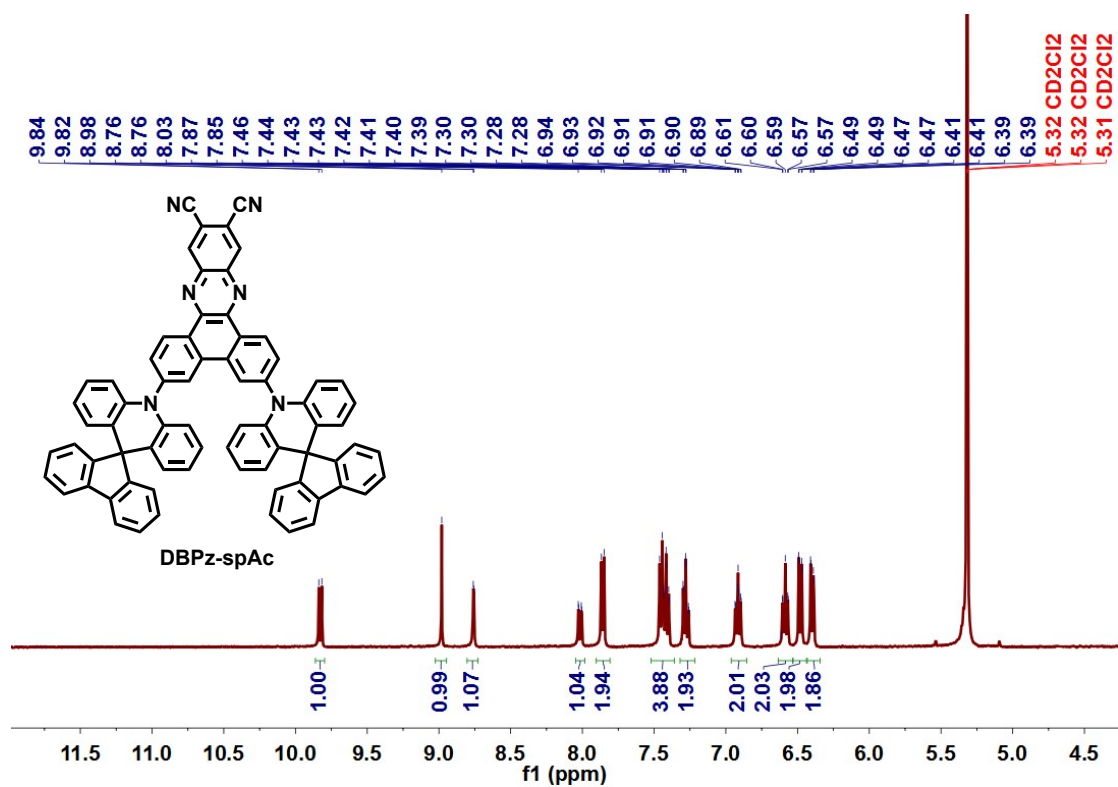


Figure S18 ¹H NMR spectrum (CD₂Cl₂, 400 MHz) of DBPz-spAc.

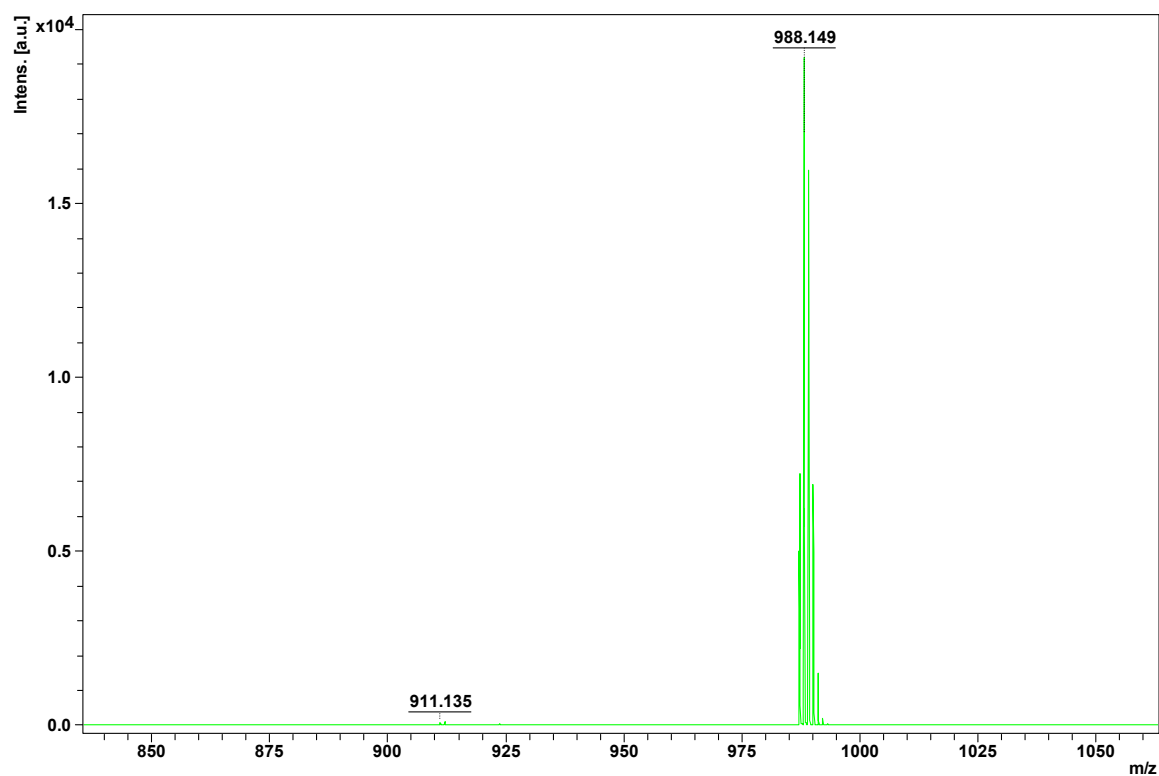


Figure S19 MALDI-TOF mass spectrum of DBPz-spAc.

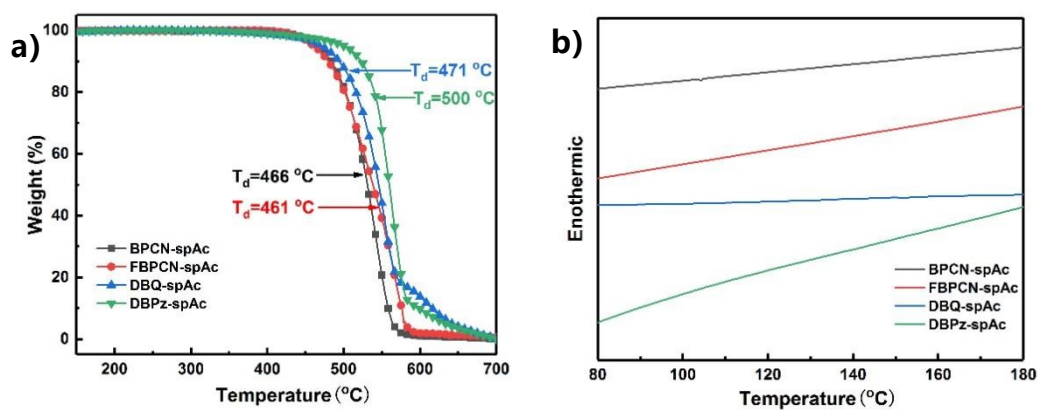


Figure S20 a) TGA and b) DSC curves of BPCN-spAc, FBPCN-spAc, DBQ-spAc, and DBPz-spAc at a heating rate of 10 °C/min under nitrogen atmosphere.

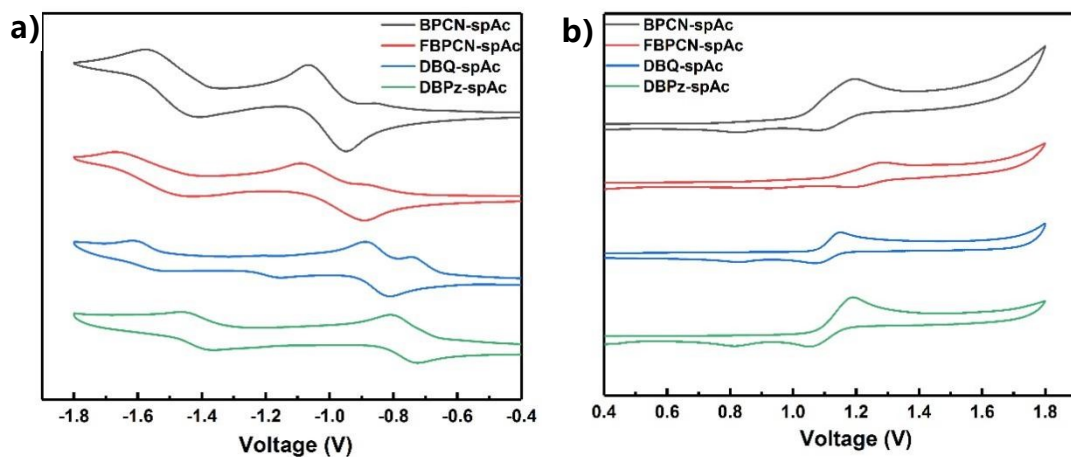


Figure S21 Cyclic voltammograms of BPCN-spAc, FBPCN-spAc, DBQ-spAc, and DBPz-spAc.

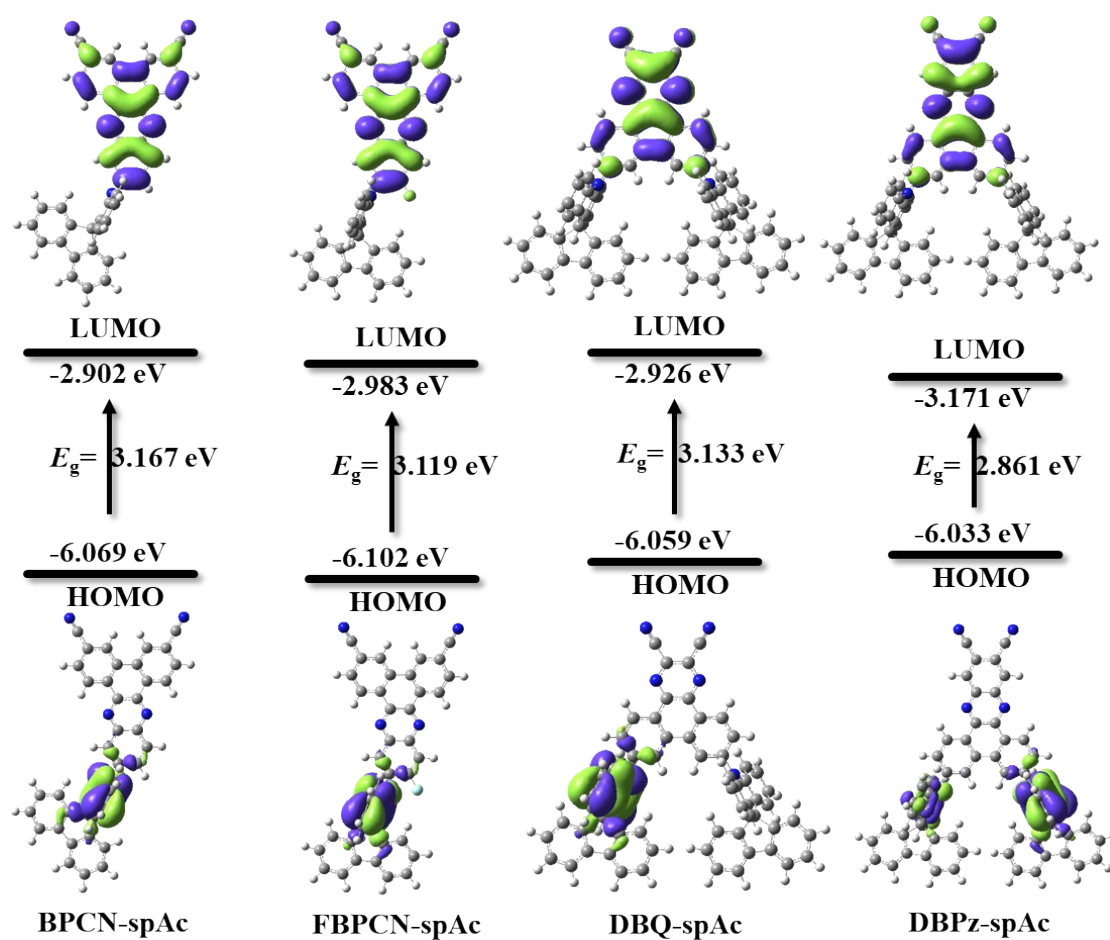


Figure S22 Energy and electron distribution of HOMOs and LUMOs for molecule in toluene (isovalue=0.02).

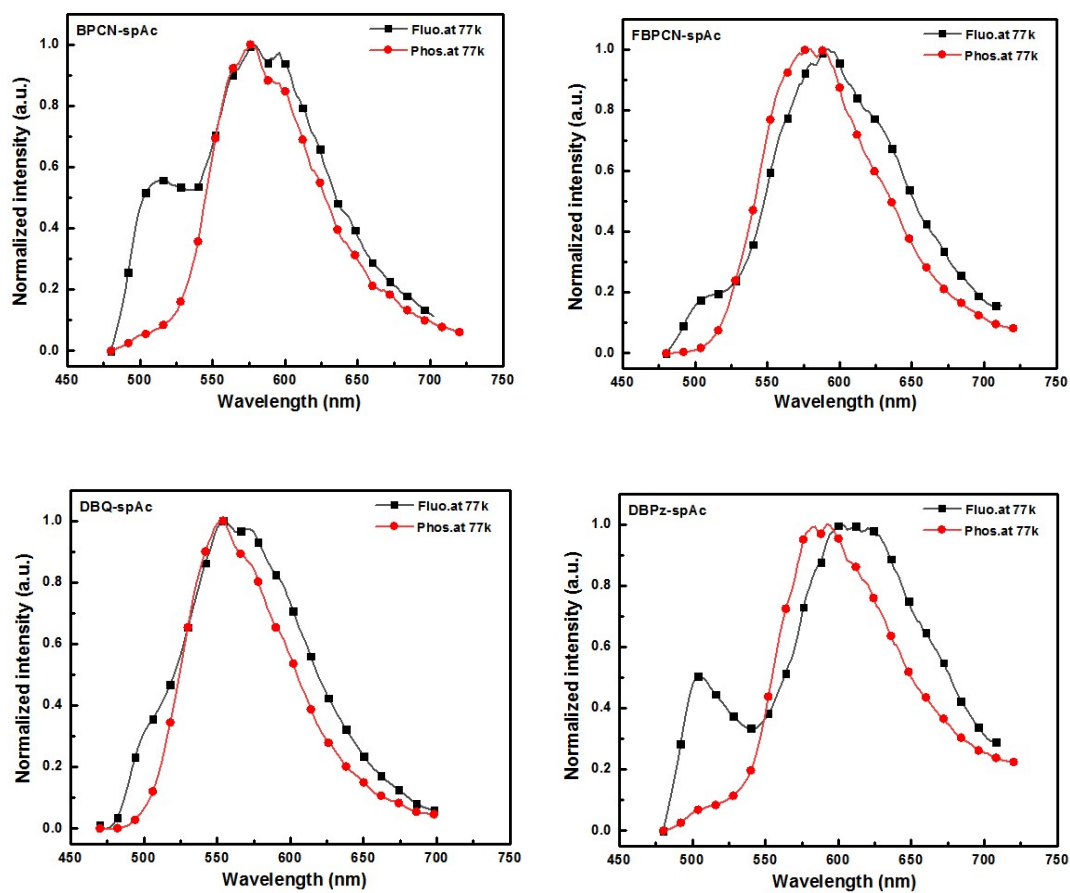


Figure S23 The PL and phosphorescence spectra of BPCN-spAc, FBPCN-spAc, DBQ-spAc and DBPz-spAc in doped films (1 wt% in CBP) at 77 K.

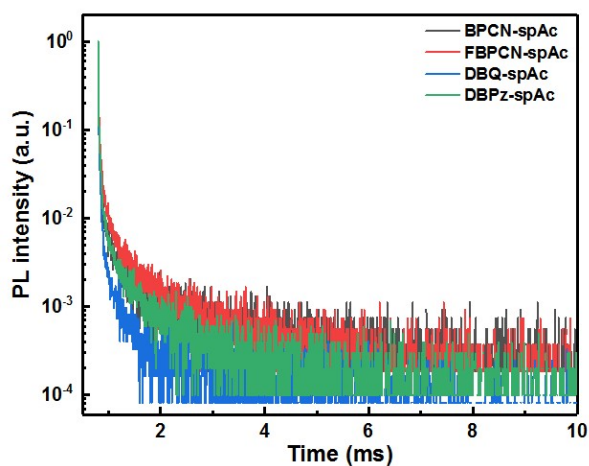


Figure S24. Transient PL decay curves in doped films (1 wt% in CBP) at 77K of BPCN-spAc, FBPCN-spAc, DBQ-spAc and DBPz-spAc.

Table S1 Detailed photophysical data of BPCN-spAc, FBPCN-spAc, DBQ-spAc and DBPz-spAc in oxygen-free toluene solution at 298 K.

Compound	Φ_{PL} ^{a)} (%)	$\Phi_{\text{p}}/\Phi_{\text{d}}$ ^{b)} (%)	τ_{p} ^{c)} (ns)	τ_{d} ^{c)} (μs)	k_{p} ^{d)} (10^6s^{-1})	k_{d} ^{e)} (10^6s^{-1})	k_{F} ^{f)} (10^6s^{-1})	k_{IC} ^{g)} (10^6s^{-1})	k_{ISC} ^{h)} (10^6s^{-1})	k_{RISC} ⁱ⁾ (10^6s^{-1})
BPCN -spAc	66.8	46.8 / 20.0	18.39	1.06	54.38	0.94	25.43	12.64	16.31	1.35
FBPCN -spAc	55.4	24.0 / 31.4	14.54	1.02	68.78	0.98	16.50	13.28	38.97	2.26
DBQ -spAc	50.2	27.6/ 22.6	21.59	0.47	46.32	2.13	12.82	12.72	20.78	3.87
DBPz -spAc	67.0	41.1 / 25.9	24.85	0.66	40.24	1.51	16.53	8.14	15.57	2.46

Table S2 Detailed photophysical data of BPCN-spAc, FBPCN-spAc, DBQ-spAc and DBPz-spAc in CBP (1 wt%) at 298 K.

Compound	$\Phi_{PL}^a)$ (%)	$\Phi_p/\Phi_d^b)$ (%)	$\tau_p^c)$ (ns)	$\tau_d^c)$ (μ s)	$k_p^d)$ ($10^6 s^{-1}$)	$k_d^e)$ ($10^6 s^{-1}$)	$k_F^f)$ ($10^6 s^{-1}$)	$k_{IC}^g)$ ($10^6 s^{-1}$)	$k_{ISC}^h)$ ($10^6 s^{-1}$)	$k_{RISC}^i)$ ($10^6 s^{-1}$)
BPCN-spAc	98.2	38.0/60.2	23.35	4.92	42.83	0.20	16.30	0.30	26.23	0.52
FBPCN-spAc	95.5	24.7/70.8	30.15	4.79	33.17	0.21	8.19	0.38	24.59	0.81
DBQ-spAc	91.0	24.8/66.2	70.74	2.51	14.14	0.40	3.51	0.35	10.28	1.46
DBPz-spAc	94.8	19.4/75.4	25.00	2.88	40.00	0.35	7.78	0.43	31.79	1.69

a) Absolute PLQY measured by using an integrating sphere under a nitrogen atmosphere and coefficient of error within $\pm 1.0\%$.

b) Prompt and delayed components of PLQY under oxygen-free conditions at room temperature.

c) The prompt and delayed fluorescence lifetimes of four emitters in oxygen-free toluene solution and doped films (1 wt% emitters in CBP) at

room temperature. d) Rate constant of prompt fluorescence (k_p), $k_p = \frac{1}{\tau_p}$. e) Rate constant of delayed fluorescence decay (k_d), $k_p = \frac{1}{\tau_d}$.

f) Rate constant of fluorescence (k_F), $k_F = \Phi_p / \tau_p$. g) Rate constant of internal conversion (k_{IC}), $\Phi_{PL} = k_F / (k_F + k_{IC})$

h) Rate constant of intersystem crossing (ISC) process ($S_1 \rightarrow T_1$) (k_{ISC}), $\Phi_p = k_F / (k_F + k_{IC} + k_{ISC})$

i) The quantum efficiencies of RISC process (k_{RISC}), $k_{RISC} = (k_p k_d \Phi_a / k_{ISC} \Phi_p)$

Table S3. Calculated spin orbit coupling constants (in cm^{-1}) between singlet and triplet excited states for BPCN-spAc, FBPCN-spAc, DBQ-spAc and DBPz-spAc in toluene.

	BPCN -spAc	FBPC N- spAc	DBQ - spAc	DBPz -spAc
$\langle S_1 \hat{H}_s T_1 \rangle$	0.018	0.020	0.059	0.083

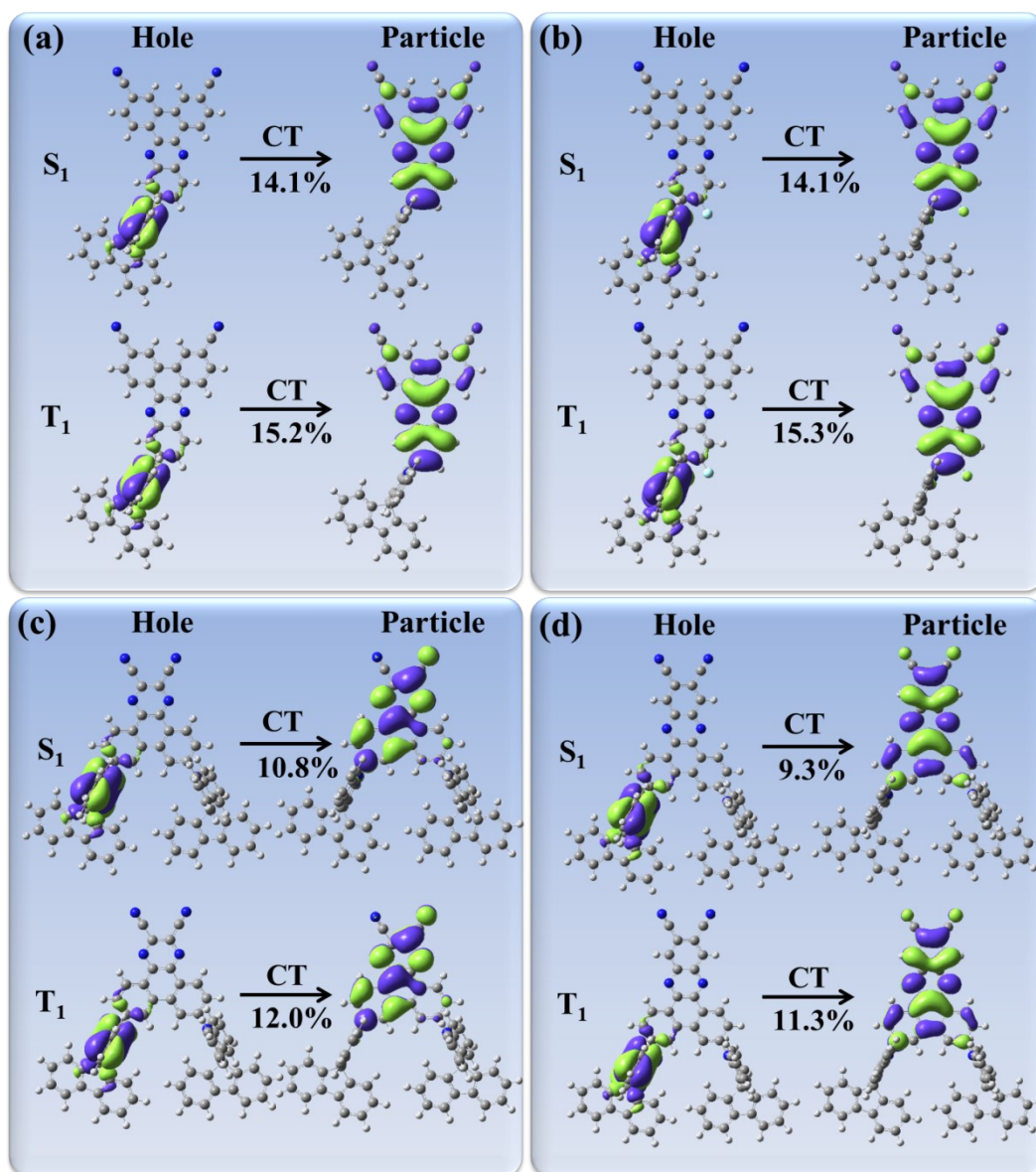


Figure S25. NTOs for singlet and triplet states of BPCN-spAc(a), FBPCN-spAc(b), DBQ-spAc(c) and DBPz-spAc(d) in toluene respectively (isovalue=0.02). The value

below every arrow represents the component of localized excitation in the corresponding transition.

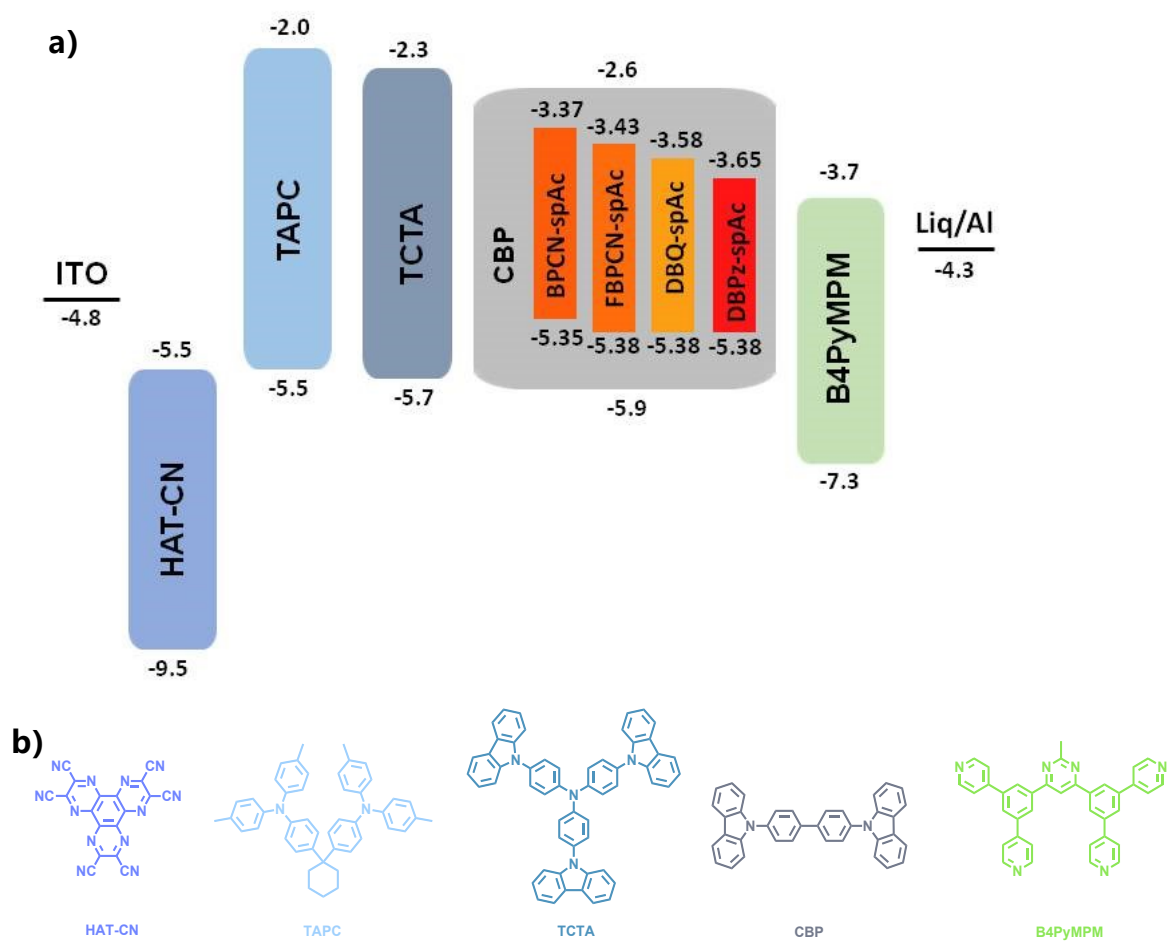


Figure S26. Energy level diagram and the chemical structures of the used materials in the devices.

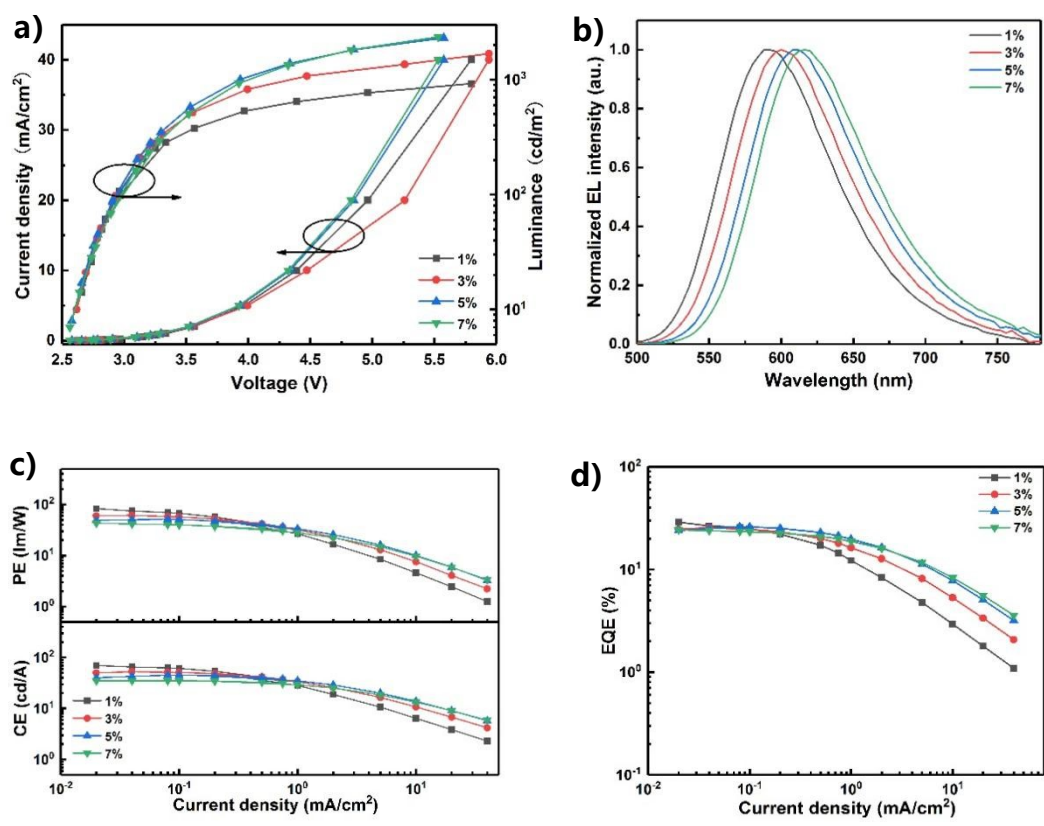


Figure S27 Device performance based on BPCN-spAc emitter: a) The current density-voltage-luminance (J-V-L) curves. b) The normalized EL spectra at 0.2 mA/cm². c) The current efficiency-current density-power efficiency (CE-J-PE) curves. d) The external quantum efficiency versus current density (EQE-J) curves.

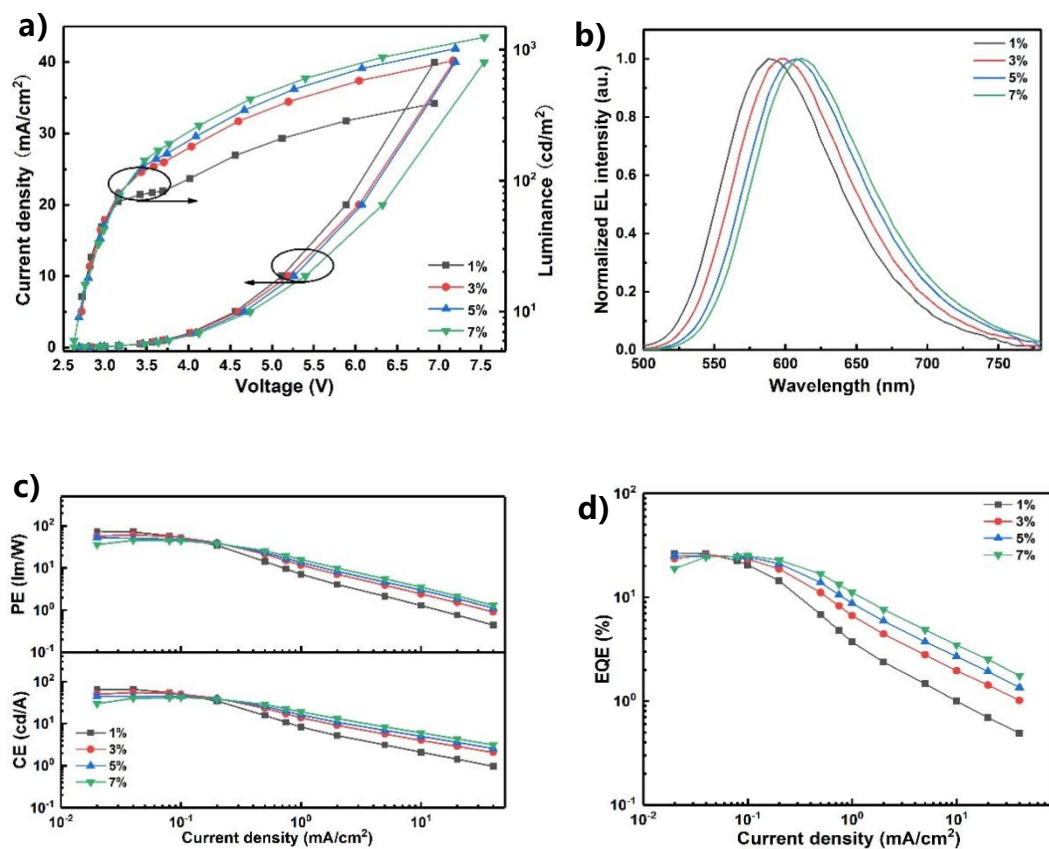


Figure S28 Device performance based on FBPCN-spAc emitter: a) The current density-voltage-luminance (J-V-L) curves. b) The normalized EL spectra at $0.2 \text{ mA}/\text{cm}^2$. c) The current efficiency-current density-power efficiency (CE-J-PE) curves. d) The external quantum efficiency versus current density (EQE-J) curves.

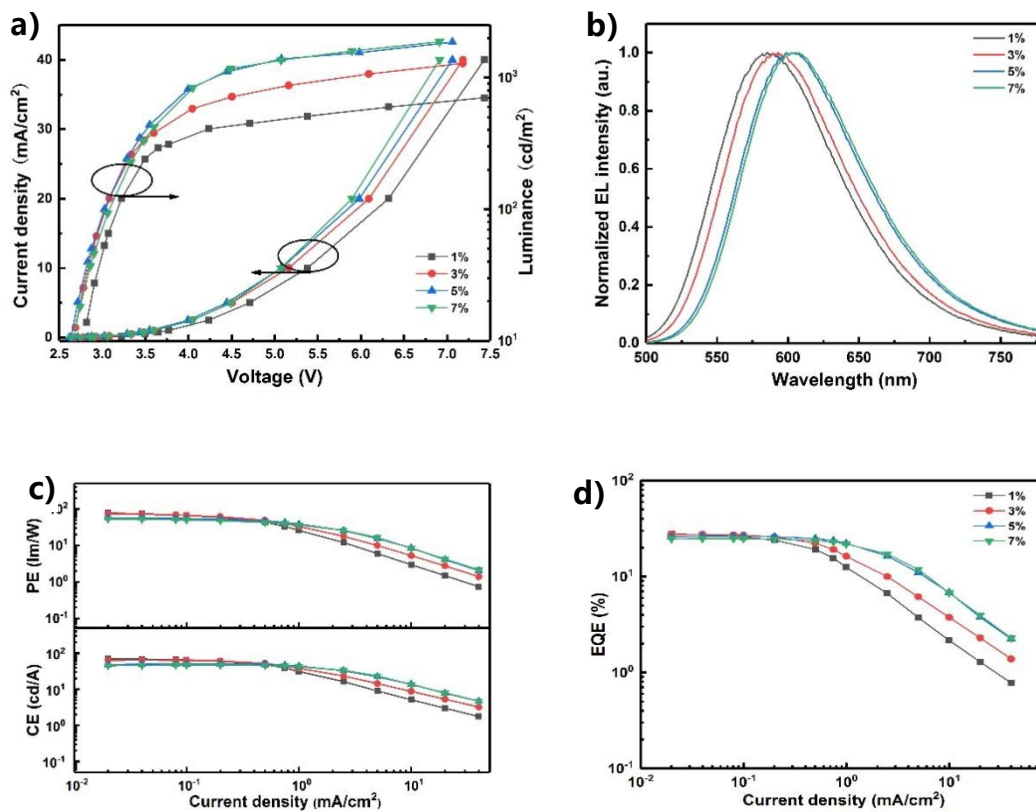


Figure S29 Device performance based on DBQ-spAc emitter: a) a) The current density-voltage-luminance (J-V-L) curves. b) The normalized EL spectra at $0.2 \text{ mA}/\text{cm}^2$. c) The current efficiency-current density-power efficiency (CE-J-PE) curves. d) The external quantum efficiency versus current density (EQE-J) curves.

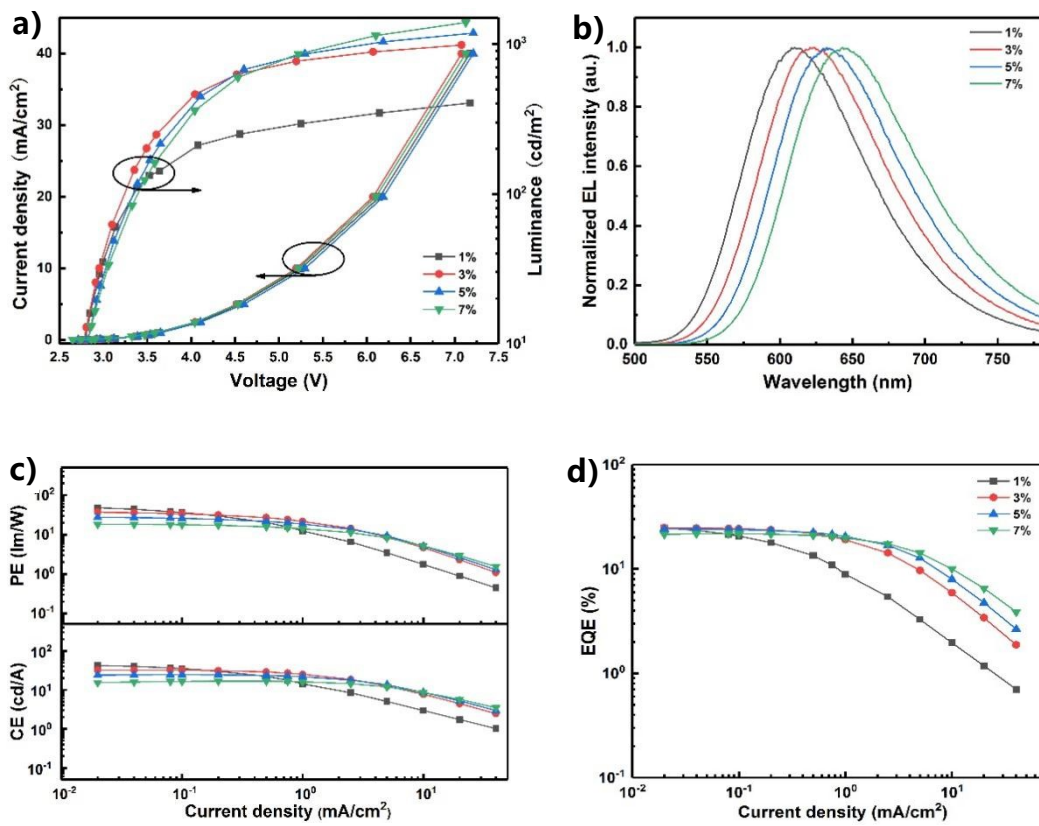


Figure S30 Device performance based on DBPz-spAc emitter: a) The current density-voltage-luminance (J-V-L) curves. b) The normalized EL spectra at $0.2 \text{ mA}/\text{cm}^2$. c) The current efficiency-current density-power efficiency (CE-J-PE) curves. d) The external quantum efficiency versus current density (EQE-J) curves.